HOKKAIDO UNIVERSITY

Title	Tumor-infiltrating DCs suppress nucleic acid-mediated innate immune responses through interactions between the receptor TIM-3 and the alarmin HMGB1
Author(s)	Chiba, Shigeki; Baghdadi, Muhammad; Akiba, Hisaya; Yoshiyama, Hironori; Kinoshita, Ichiro; Dosaka-Akita, Hirotoshi; Fujioka, Yoichiro; Ohba, Yusuke; Gorman, Jacob V.; Colgan, John D.; Hirashima, Mitsuomi; Uede, Toshimitsu; Takaoka, Akinori; Yagita, Hideo; Jinushi, Masahisa
Citation	Nature Immunology, 13(9), 832-842 https://doi.org/10.1038/ni.2376
Issue Date	2012-09
Doc URL	http://hdl.handle.net/2115/52108
Type	article (author version)
Additional Information	There are other files related to this item in HUSCAP. Check the above URL.
File Information	NI13-9_832-842.pdf

Instructions for use

Hokkaido University Collection of Scholarly and Academic Papers : HUSCAP

Tumor-infiltrating DCs suppress nucleic acid–mediated innate immune responses through interactions between the receptor TIM-3 and the alarmin HMGB1

Shigeki Chiba [1], Muhammad Baghdadi [1, 3, 4], Hisaya Akiba [6], Hironori Yoshiyama [1], Ichiro Kinoshita [4], Hirotoshi Dosaka-Akita [4], Yoichiro Fujioka [5], Yusuke Ohba [5], Jacob V. Gorman [7], John D. Colgan [7], Mitsuomi Hirashima [8], Toshimitsu Uede [2], Akinori Takaoka [3], Hideo Yagita [6], Masahisa Jinushi [1]

[1] Research Center for Infection-Associated Cancer, [2] Division of Molecular Immunology, [3] Division of Signaling on Cancer and Immunology, Institute for Genetic Medicine, Hokkaido University, Sapporo, 060-0815, Japan.

[4] Department of Medical Oncology, [5] Department of Pathophysiology and Signal Transduction, Hokkaido University Graduate School of Medicine, Sapporo, 060-0815, Japan.

[6] Department of Immunology, Juntendo University School of Medicine, Tokyo, 113-8421, Japan

[7] Department of Internal Medicine, University of Iowa, Iowa City, IA, 52242, USA

[8] Department of Immunology and Immunopathology, Faculty of Medicine, Kagawa University, Kita-gun, Kagawa, 761-0791, Japan

Key words: TIM-3, HMGB1, Nucleic acids, Innate immunity, Dendritic cells

Abstract

The mechanisms by which tumor microenvironments modulate nucleic acid-mediated innate immunity remain unknown. Here, we identified the receptor TIM-3 as key to circumventing the stimulatory effects of nucleic acids in tumor immunity. TIM-3 is highly expressed on tumor-associated dendritic cells (DC) in murine tumors and cancer patients. DC-derived TIM-3 suppresses innate immune responses through Toll-like receptor and cytosolic sensor recognition of nucleic acids *via* a galectin-9 independent mechanism. Instead, TIM-3 interacts with the HMGB1 to interfere with recruitment of nucleic acids into DC endosomes and attenuates the therapeutic efficacy of DNA vaccination and chemotherapy by reducing immunogenicity of nucleic acids released from dying tumor cells. Together, these findings define a novel mechanism by which tumor microenvironments suppress antitumor immunity mediated by nucleic acids.

Accumulating evidence demonstrates the important potential of endogenous immune responses in modulating the clinical outcome of malignant diseases[1, 2]. Thus, manipulation of the immune system should enable enhancement the therapeutic effects of current anticancer modalities [3, 4]. On the other hand, oncogenic and epigenetic alterations of tumor cells frequently adopt multiple strategies to form complex networks with tumor-infiltrating immune cells, leading to the impairment of efficient tumor immunosurveillance [5, 6].

Innate immunity serves as a first line of defense against infectious agents, and germ-line-encoded pattern recognition receptors (PRR) detect stressed and infected cells and elicit potent effector activities that accomplish efficient microbe containment [7]. Among the specialized subsets of innate immune cells, dendritic cells (DC) are particularly important as critical sensors through their wide expression of different PRR [8]. These pattern-sensing systems on DC are also applicable to the recognition of tumor-derived stress-related factors. In particular, Toll-like receptors (TLR) and cytosolic sensors for DNA and RNA recognition expressed by DC utilize endogenous host elements carrying microbial components (e.g. HMGB1), pathogen-associated molecular patterns (PAMPs), and/or nucleic acids to stimulate intrinsic apoptotic pathways to generate protective immune responses against nascent tumors [9-11]. However, it remains largely

unknown how DC regulate PRR-mediated innate immune systems within tumor microenvironments and thereby how they affect anticancer therapies.

In this study, we identify T cell Ig- and mucin-domain-containing molecule-3 (TIM-3) on DC as a key factor in circumventing nucleic acid-mediated innate immune activation. TIM-3 was initially identified as a negative regulator of T_H1 immunity upon ligation with galectin-9 [12-14]. However, TIM-3 is also expressed on myeloid cells such as monocytes and macrophages [15, 16], but whether TIM-3 on DC has a role in the regulation of antitumor immunity has remained largely unknown. We found here that TIM-3 levels are up-regulated in DC in tumor microenvironments. Furthermore, TIM-3 on tumor-associated dendritic cells (TADC) suppresses PRR-mediated innate immune responses to nucleic acids by interfering with HMGB1-mediated activation of nucleic acid sensing systems. These findings define a novel mechanism by which tumor microenvironments impede immune responses of DC to nucleic acid adjuvants, resulting in impaired antitumor immunosurveillance and therapy.

RESULTS

High expression of TIM-3 in tumor-infiltrating DC

To explore a potential role for TIM-3 in regulating anti-tumor responses we examined its expression on myeloid cells from mice bearing 3LL and MC38 tumors. Single cell suspensions prepared from subcutaneous tumors revealed high TIM-3 expression on $CD11c^{hi}$ conventional DC (cDC), $CD11c^{lo}B220^{+}PDCA1^{+}$ plasmacytoid DC (pDC) and $CD11b^{+}F4/80^{+}$ tumor-associated macrophages (TAM) but not on $CD11b^{+}Gr\text{-}1^{+}$ myeloid-derived suppressor cells (MDSC) (Fig. 1a and Supplementary Fig. 1a). In contrast, few TIM-3-expressing DC or macrophages were found in the tumor-draining or distal lymph nodes and spleen of tumor-bearing mice, or in mice without tumors (Fig. 1a). In line with tumor-specific expression of TIM-3, we also detected TIM-3 on tumor cells *in situ* and tumor-infiltrating, but not splenic, $CD8^{+}$ T cells of tumor-bearing mice. In contrast, TIM-3 was not detected on *in vitro* cultured murine tumor cell lines, indicating that tumor microenvironments may play a role in the regulation of TIM-3 expression on both the tumor and on host leucocytes (Supplementary Fig. 1b and c). However, TIM-3 was expressed on *in vitro* cultured human NSCLC (non-small cell lung carcinoma) tumor lines and primary $EpCAM^{+}$ NSCLC epithelial tumor cells from cancer patients (Supplementary Fig. 1d and e). TIM-3 was upregulated in TADC at much higher levels

and earlier time points than on tumor-infiltrating $CD8^+$ T cells after subcutaneous tumor challenge (Fig. 1b). In contrast, TIM-3 expression in $CD8^+$ T cells gradually increased and reached maximal levels (~50%) by 4 weeks after tumor challenge (Fig. 1b). These results suggest that tumor microenvironments induce DC to express TIM-3 with kinetics different from those on $CD8^+$ T cells.

To investigate possible tumor-derived factors contributing to TIM-3 upregulation by DC, we incubated immature bone marrow-derived dendritic cells (BMDC) with murine tumor cells or with tumor cell supernatants overnight. TIM-3 expression was significantly increased by either co-culture with tumor cells or treatment with culture supernatants (Fig. 1c and d). Various factors mainly derived from tumor cells and their microenvironments bestow tumorigenic activities upon DC by inducing their expression of tumor-promoting and immunosuppressive factors, such as arginase-I, IDO, IL-10, TGF-β1, and VEGF [17-19]. Although 3LL tumors treated with inhibitors individually for VEGF-R2, IL-10, or arginase-I had marginal inhibitory effects on TIM-3 expression when added to BMDC (Supplementary Fig. 2a), treatment with a combination of all three inhibitors largely diminished tumor cell supernatant-mediated upregulation of TIM-3 on BMDC (Fig.1d). Moreover, TIM-3 on BMDC was significantly up-regulated by recombinant IL-10, VEGF-A or both in a dose-dependent manner (Supplementary Fig. 2b).

In contrast, TIM-3 was not upregulated on murine 3LL NSCLC tumor cells treated with VEGF-A and IL-10, suggesting that tumor cells utilize distinct mechanisms to induce their expression of TIM-3 compared to those for DC (Supplementary Fig. 2c). Thus, TIM-3 expression on DC is regulated by the synergistic actions of multiple immunoregulatory factors released from tumor cells. In addition, we also detected high expression of TIM-3 on the cell surface of $CD11c^+$ TADC from patients with advanced NSCLC, gastric adenocarcinoma and neuroendocrine tumors but not on DC differentiated from peripheral blood monocytes (MoDC) of patients or healthy volunteers (Fig. 1e). These findings reveal that TIM-3 is specifically detected at high levels on DC from both murine and human tumor microenvironments.

TIM-3 suppresses innate responses to nucleic acids

We next evaluated the role of TIM-3 on DC function. To do so, we isolated the $TIM\text{-}3^+$ population from bulk BMDC, since TIM-3 is expressed on only a small portion of granulocyte-monocyte colony stimulating factor (GM-CSF)-differentiated BMDC (5~10%). $TIM\text{-}3^+$ DCs were composed of more mature $CD11c^{hi}CD86^{hi}$ cells compared to their $TIM3^-$ counterparts. However, their ability to cross-prime ovalbumin (OVA)-specific T cells was similar to that of the $TIM\text{-}3^-$ DC (data not shown).

Given recent reports that TIM-3 on antigen-presenting cells coordinates with TLR signals to trigger inflammatory signals [15], we examined the role of TIM-3 in the regulation of TLR-mediated innate immune responses. Protein expression of the cytokines IFN-β1, IFN-α4, IL-6 and IL-12 in TIM-3$^+$ DC isolated from wild-type BMDC were much lower than that of BMDC isolated from TIM-3-deficient mice (*Tim3*$^{-/-}$ also known as *Havcr2*$^{-/-}$) upon stimulation with nucleic acid agonists for TLR3 (poly (I: C)), TLR7 (R848) and TLR9 (CpG-ODN) but not TLR2 (peptidoglycan, PGN) or TLR4 (LPS) (Fig. 2a and Supplementary Fig. 3a). Since TLR3, TLR7 and TLR9 serve as pattern recognition sensors for double-strand RNA, single-strand RNA and single-strand DNA, respectively, we hypothesized that TIM-3 might be broadly involved in the regulation of nucleic acid-mediated immune responses. Indeed, cytokine secretion by TIM-3$^+$ BMDC was much lower than from *Tim3*$^{-/-}$ mice upon stimulation with poly (dA:dT) (B-DNA) or interferon stimulatory DNA (ISD) which are ligands for the cytosolic DNA sensor as well as poly (I: C) or triphosphate (3p)-RNA which are ligands for the RNA sensor MDA5 or RIG-I (Fig. 2a). Moreover, treatment with anti-TIM-3 monoclonal antibody (mAb) or small interfering RNA targeting TIM-3 resulted in a marked upregulation of IFN-β protein in TIM-3$^+$ wild-type DC in response to agonists for cytosolic sensors or TLR (Fig. 2b). TIM-3 blockade also augmented IFN-β1 expression in TIM-3$^+$ DC derived from wild-type but not TIM-3-deficient mice upon stimulation with plasmid DNA encoding either melanoma

antigens tyrosinase-related protein-2 (TRP-2), gp100 or plasmid with no insert, indicating that the tumor antigen-encoding sequence was dispensable for the DNA-induced innate immune responses (Fig.2c and data not shown).

To delineate the contribution of TIM-3 to nucleic acid-mediated innate immune responses, we transfected TIM-3-negative mouse embryonic fibroblasts (MEF) with a control or TIM-3-expressing vector. TIM-3 expression led to decreased cytokine production by MEF in response to B-DNA, genomic DNA isolated from tumors (B16 and EL-4) or pathogens including *Escherichia coli, Helicobacter pylori* and human cytomegalovirus (Fig. 2d and Supplementary Fig. 3b). The TIM-3-mediated suppression of innate responses to bacterial and viral DNA was also observed in BMDC (data not shown). Moreover, the luciferase reporter assays revealed that TIM-3 suppressed the B-DNA-induced transcriptional activities of IRF-3 and NF-κB in HEK293 cells, which serve as essential components of TLR and cytosolic sensor-mediated responses (Fig. 2e).

To examine whether TIM-3 negatively regulates innate immune responses to nucleic acids *in vivo*, the mRNA levels of IFN-β1 and IL-12 were examined in TADC isolated from tumor-bearing mice or cancer patients. IFN-β1 and IL-12 transcription and protein secretion induced by plasmid DNA was reduced in TADC compared to splenic DC or MoDC, but treatment with

anti-TIM-3 mAb increased cytokine expression and release by TADC even to a level even higher than that seen in splenic DC or MoDC (Fig. 2f and g).

Consistent with a critical role for DC-derived TIM-3 in restraining immune responses to nucleic acids, TIM-3 strongly suppressed cytokine production by $CD11c^{lo}B220^{+}$ pDC in a manner comparable to that seen with $CD11c^{hi}$ cDC infiltrating into tumor tissue. Anti-TIM-3 mAb-mediated upregulation of IFN-β and IL-12 was much greater in $CD11c^{hi}$ DC or $CD11c^{lo}B220^{+}$ pDC than TAM or MDSC isolated from tumor tissue, while TIM-3 upregulation was comparable among these myeloid lineage cells (Supplementary Fig. 1a and 3c). The TIM-3 blockade had little effect on innate responses in TIM-3^{hi} tumor-infiltrating $CD8^{+}$ T cells upon stimulation with CpG-ODN (data not shown). Together, these results demonstrate that TIM-3 substantially reduces the activation of TADC by interfering with their recognition and response to normally immunostimulatory nucleic acids.

DC-specific **TIM-3 compromises antitumor efficacy of DNA**

To examine the impact of TIM-3 on nucleic acid-mediated antitumor responses, we utilized various nucleic acid-based adjuvants, including DNA plasmids encoding control or melanoma antigens (TRP2) [20] as well as TLR9 agonists (CpG-ODN), as therapeutic options against established murine tumors. Immunization with DNA partially reduced tumor burden caused by

B16-F10 melanomas. Although anti-TIM-3 mAb alone afforded a small delay of tumor growth, it eventually failed to protect mice from succumbing tumors (Fig. 3a). In contrast, combined treatments with DNA and anti-TIM-3 mAb resulted in a marked growth inhibition (Fig. 3a and data not shown). These results suggest that TIM-3 exerts a marginal effect because endogenous DNA released in untreated tumors is limited, but exogenous DNA administered therapeutically could trigger a strong antitumor effect upon TIM-3 blockade. TIM-3 blockade delayed tumor growth to a similar extent in combination with either control plasmid DNA with no insert or TRP2-encoding DNA, suggesting that TIM-3 regulates innate immune responses independently of a particular tumor antigen (data not shown). Consistent with this notion, TIM-3 blockade induced the antitumor activities of TRP2-DNA but not peptide vaccines (Fig. 3a and data not shown). The protein levels of IFN-β and IL-12 were higher in tumors from mice treated with plasmid DNA and anti-TIM-3 mAb than those treated with anti-TIM-3 mAb or DNA alone, indicating the close relationship between cytokine levels and antitumor effects (Fig. 3b).

To further define the role of DC-derived TIM-3 in circumventing the therapeutic efficacy of DNA vaccines, B16-F10 melanomas were treated with plasmid DNA and anti-TIM-3 mAb in CD11c-DTR mice in which conditional depletion of $CD11c^{+}$ DC can be achieved by administration of diphtheria toxin (DT). DNA and anti-TIM-3 mAb protected mice from growing tumors compared to DNA alone in endogenous $TIM\text{-}3^{hi}$ TADC-bearing control mice.

In contrast, the depletion of DC in CD11c-DTR mice markedly increased the antitumor effects of DNA alone in this model (Fig. 3C). To elucidate whether TIM-3 on DC may impede antitumor responses mediated by nucleic acids, BMDCs generated from wild-type or TIM-3-deficient mice were adoptively transferred into DC-deficient CD11c-DTR mice with B16 melanoma. Treatment with plasmid DNA was ineffective against established B16-F10 tumors in the presence of wild-type DCs, whereas the treatment with DNA induced profound inhibition of tumor growth following transfer of TIM-3-deficient DCs (Fig. 3d).

To further define the role of TIM-3 expressed on endogenous DC in the antitumor effect of DNA adjuvant, we generated mixed BM chimeric mice in which TIM-3-expressing DC from CD11c-DTR mice could be selectively depleted. BM cells from TIM-3-deficient mice and CD11c-DTR (TIM-3-KO + CD11c-DTR) mice were mixed at a 1:1 ratio and used to reconstitute irradiated WT recipient mice, and the antitumor effects of DNA were compared in TIM-3-KO + CD11c-DTR BM chimeras. DNA treatment alone potently restrained tumor growth in DT-treated TIM-3-KO + CD11c-DTR BM chimeras compared to those without DT, whereas anti-TIM-3 mAb had an inhibitory effect on tumor growth irrespective of DT treatment in TIM-3-KO + CD11c-DTR mice (Fig. 3e). Together, these findings further exemplify the role of DC-specific TIM-3 in negatively regulating nucleic acid-mediated antitumor immunity. The synergistic antitumor effects of DNA and anti-TIM-3 mAb were similarly observed in NOD-

SCID mice and C57BL/6 mice treated with anti-CD8 depleting Ab or control Ig (Supplementary Fig. 4). These results further confirm that TIM-3 on $CD8^+$ T cells is not responsible for the synergistic activities of DNA and anti-TIM3 mAb, which differs from previous observations suggesting that $CD8^+$ T cells are necessary for exerting antitumor responses induced by anti-TIM-3 mAb alone [21].

To examine the mechanisms by which TIM-3 blockade elicits antitumor responses, we focused on the contributions of type-I IFN and IL-12 in the nucleic acid-triggered responses because these are well known antitumor effector cytokines. Indeed, the antitumor effect of DNA was mostly abolished in DT-treated CD11c-DTR mice when administered with neutralizing mAb for type-I IFN receptor (IFN-IR) and IL-12. Moreover, the antitumor effect of anti-TIM-3 mAb and DNA was also abrogated in DT-untreated CD11c-DTR or NOD-SCID mice by the combined blockade of IFN-IR and IL-12 (Fig. 4a-c). The treatment with neutralizing Abs for IFN-I and IL-12 had little impacts on B16-F10 tumor growth in the absence of DNA administration, indicating that the immunogenic DNA is necessary for exerting tumor immunosurveillance by IFN-I and IL-12 (data not shown).

$CD11c^{lo}$ $B220^+$ $PDCA1^+$ pDC, $CD11c^{hi}$ cDC, $F4/80^+$ $CD11b^+$ macrophages and $CD45^-$ $gp38^+$ stromal cells were the major producers of type-I IFN and IL-12 within the tumor microenvironments of NOD-SCID mice upon treatment with DNA and anti-TIM-3 mAb (Fig.

4d). Moreover, the cytotoxic activities were markedly increased in NK cells, macrophages and pDC of NOD-SCID mice treated with DNA and anti-TIM-3 mAb (Fig. 4e). These results are consistent with previous reports that appropriate innate immune adjuvants may trigger tumor-killing effector functions of pDC [22]. In the case of DC-depleted CD11c-DTR mice, the main sources of IFN-β1 and IL-12 were macrophages and CD45- stromal cells, and NK cells and macrophages were major effectors involved in killing tumor cells in an IFN-IR and IL-12-dependent manner (data not shown).

Together, these results suggest that TIM-3 blockade might convert tolerogenic innate cells into antitumor effectors, and type-I IFN and IL-12 as well as various innate cells act as downstream effectors to trigger antitumor responses mediated by DNA and anti-TIM-3 mAb.

TIM-3 regulation of innate responses is Galectin-9-independent

The interaction between galectin-9 and TIM-3 on myeloid cells elicits antimicrobial and antitumor immunity but inhibits T_H1 responses [23-25]. However, treatment with recombinant galectin-9 or anti-galectin-9 mAb did not suppress B-DNA-mediated cytokine production in $TIM\text{-}3^+$ or $TIM\text{-}3^-$ DC (Fig. 5a and b). Galectin-9 mRNA was detected at much lower levels in TADC and tumor cells as compared to splenic DC derived from tumor-bearing or normal mice (Fig. 5c). Galectin-9 levels were also significantly lower in bulk tumor tissues compared to

normal tissues in B16 tumor-bearing mice, implying that galectin-9 production was compromised in tumors (Fig. 5d). Furthermore, treatment with anti-galectin-9 mAb did not increase the antitumor effects of plasmid DNA (Fig. 5e).

Phosphatidylserine (PS) exposed by apoptotic cells is another ligand for TIM-3 [26, 27]. However, treatment with annexin-V, which also binds PS and potentially competes with TIM-3 – had little effect on B-DNA-mediated IFN-β1 gene expression in TIM-3$^+$ MEF (Fig. 5f), suggesting that TIM-3-mediated regulation of nucleic acid-sensing is independent of the recognition of PS on apoptotic cells. Together, these findings demonstrate that DC-derived TIM-3 recognizes a ligand other than galectin-9 or PS to suppress nucleic acid-mediated immune responses.

TIM-3 serves as a receptor for HMGB1

In HEK293 cells, B-DNA is recognized by RIG-I through the induction of an RNA polymerase III-transcribed RNA intermediate [28]. TIM-3 had little inhibitory effect on the IFN-β1 response in HEK293 cells stimulated with expression vectors for the intracellular receptor RIG-I or the signaling adapters STING, MAVS, MyD88 and TRIF (data not shown), indicating that TIM-3 acts on the nucleic acids-sensing systems upstream of PRR-specific pathways.

High mobility group box-1 (HMGB1) is an evolutionarily conserved nuclear protein that

evokes pleiotropic functions in various physiological and pathological situations [29]. HMGB1 also has an essential role in activating nucleic acid sensor-mediated innate immune responses [30, 31], we therefore examined HMGB1 for a potential interaction with TIM-3. We could indeed find that TIM-3 bound HMGB1 with an affinity comparable to that of RAGE, a known HMGB1 receptor (Fig. 6a). Furthermore, the interaction between HMGB1 and TIM-3 was partially suppressed in the presence of RAGE-Fc or galectin-9 proteins (Supplementary Fig. 5a), confirming the specificity of HMGB1 and TIM-3 in this analysis.

TIM-3 binds PS through a metal ion–dependent ligand binding site (MILIBS) in the FG loop [32, 33]. We therefore constructed a mutated TIM-3-Fc protein with amino acid Gln62 near the FG loop changed to Ala (Q62A) at the galectin-9–independent ligand binding site [32]. Substitution of Gln62 with Ala largely abrogated the ability of TIM-3 to bind HMGB1, implying that the MILIBS portion of TIM-3 is critical for HMGB1 binding. In addition, the interaction of TIM-3-Fc with HMGB1 was blocked by anti-TIM-3 mAb (Fig. 6b).

HMGB1 has DNA-binding domains within its A-box and B-box, and its interaction with DNA is enhanced by the tail domain at its C terminus [29]. Thus, we examined whether TIM-3 and nucleic acids might compete for binding to the same domain of HMGB1. Indeed, the binding of either B-DNA or TIM-3-Fc to HMGB1 was mostly abrogated by deletion of the A-box, but not

B-box or C-terminal domain (Supplementary Fig. 5b and c). Furthermore, the binding of biotin-labeled B-DNA to HMGB1 was inhibited by unlabeled TIM-3-Fc in a concentration-dependent manner. In contrast, the mutant TIM-3 protein Q62A failed to inhibit the interaction between B-DNA and HMGB1 compared to the control Flt3L-Fc (Fig. 6c), implying that TIM-3 and nucleic acids compete with each other for the binding to A-box domain of HMGB1.

Moreover, TIM-3^+ DC interact with biotin-labeled HMGB1 with a higher affinity than do TIM-3^- DC, although both were inhibited by anti-TIM-3 mAb (Fig. 6d). The binding of HMGB1 to TIM-3^- DC was detectable, though much lower than the binding to TIM-3^+ counterparts, suggesting that some other receptors such as RAGE may be involved in the HMGB1 binding to TIM-3^-DC (Fig. 6d). TIM-3 was also colocalized with HMGB1 in TIM-3^+DC (Fig. 6e), and bound to HMGB1 in TIM-3-transfected MEFs. Furthermore, the densitometry of immunoprecipitated bands revealed that the inhibitory effect of anti-TIM-3 mAb on this binding was statistically significant (Fig. 6f). HMGB1 mRNA levels were significantly higher in tumors than normal tissues, implying that in contrast to galectin-9, HMGB1 production occurred in tumors (Fig. 6g). Taken together, these results reveal TIM-3 as a putative receptor for HMGB1 in DC in tumor microenvironments.

TIM-3 inhibits recruitment of nucleic acids into endosomes

Proper trafficking of nucleic acids into endosomal vesicles is a key event in the initiation of innate immune signaling. Danger-associated molecules such as uric acids and HMGBs complex with nucleic acids and allow them access to endosomal vesicles and triggering of immune responses [34]. We therefore examined whether HMGB1 directly affects recruitment of nucleic acids into endosomal vesicles. To do so, we adopted an experimental system utilizing HMGB1-KO MEFs loaded with recombinant HMGB1 proteins. Consistent with the role of HMGB1 in mediating immune sensing of nucleic acids, the addition of HMGB1 facilitated transfer of B-DNA into early endosomal marker EEA1-positive endosomal vesicles in HMGB1-KO MEFs compared to controls (Fig. 7a).

In contrast, B-DNA was mainly located around the plasma membrane, but the recruitment of B-DNA into endosomal vesicles was decreased substantially in TIM-3-GFP-transfected HMGB1-KO MEFs upon stimulation with HMGB1, suggesting that TIM-3 interferes with HMGB1-dependent endosomal transfer of nucleic acids (Fig. 7a).

To further examine whether endogenous TIM-3 has an inhibitory effect on nucleic acid recruitment to endosome, TIM-3$^+$wild-type or TIM-3-deficient DC were utilized to evaluate endosomal localization of nucleic acid ligand such as B-DNA or CpG-ODN. A significant portion of nucleic acids was preferentially localized in endosomal vesicles in TIM-3-deficient DC compared to TIM-3$^+$ wild-type DC upon stimulation with nucleic acids and HMGB1 (Fig.

7b and data not shown).

We next quantify the amounts of B-DNA in total and EEA1$^+$ early endosomal vesicles in TIM-3$^+$ and TIM-3$^-$ DC using image-processing software as described previously [35]. B-DNA was lower in the EEA1$^+$ endosomal vesicles of TIM-3$^+$ DC compared to those of TIM-3$^-$ DC, while total amounts of B-DNA was comparable in both populations (Fig. 7c). Consistent with these findings, TIM-3 was mainly colocalized with HMGB1 in EEA1$^+$ endosomal vesicles in TIM-3$^+$DC upon HMGB1 stimulation (Fig. 7d).

To further substantiate the differences of DNA recruitment into endosomal vesicles in TIM-3$^+$ and TIM-3$^-$ cells, we purified endosomal vesicles by subcellular fractionation to measure the recruitment of DNA in TIM-3$^+$ or TIM-3$^-$ DC. We confirmed that the markers for early endosome (EEA1), late endosome (Rab7) and transferring receptor (TfR) was similarly expressed in the TIM-3$^+$ DC and TIM-3$^-$DC (Fig. 7e). As expected, the dot blot analysis revealed that B-DNA was detected in purified early or late endosomal vesicles from TIM-3$^+$ DC at much lower levels than those from TIM-3$^-$ DC, whereas B-DNA was detected in the heavy membrane fractions of TIM-3$^+$ DC at higher levels than TIM-3$^-$counterparts. There was little difference in the amounts of endocytosed DNA in the total and light plasma membrane fractions (Fig. 7e). Moreover, the uptake of B-DNA was lower in the endosomal vesicles purified from HMGB1-stimulated TIM-3$^+$ DC compared to those of TIM-3$^-$ DC, as quantified by flow

cytometry (Supplementary Fig. 6). Together, these results reveal a role for TIM-3 in restraining transport of nucleic acids to endosome, which is normally triggered by HMGB1.

We further examined the involvement of HMGB1 in TIM-3-mediated suppression by using HMGB1-deficient MEF. TIM-3 transfection had little inhibitory effect on cytokine production by HMGB1-deficient MEF upon stimulation with B-DNA, but the addition of recombinant HMGB1 protein restored TIM-3-mediated suppression (Fig. 7f). Furthermore, treatment with anti-HMGB1 neutralizing Ab abrogated the nucleic-acid-mediated responses evoked by TIM-3 blockade in TIM-3^+ DC to control levels (Fig. 7g). Together, these findings reveal that TIM-3 may negatively regulate HMGB1-mediated activation of the innate immune response to nucleic acids.

TIM-3 suppresses the antitumor effects of chemotherapy

Recent works have illustrated that some cytotoxic therapies may induce a form of immunogenic cell death in which the release of danger-associated molecules such as HMGB1 from dying tumor cells provides an endogenous adjuvants [36, 37]. In addition, recent evidence has revealed that the immunogenicity of cancer vaccines is boosted in conjunction with nucleic acid released from dying tumors, engendering the generation of protective antitumor immunity [38]. We therefore hypothesized that TIM-3-mediated regulation of nucleic acid-sensing systems may

modulate antitumor immunity induced by chemotherapy-mediated “immunogenic cell death”. To define the role of DC-derived TIM-3 in restraining cytotoxic agent-induced innate immune responses, TIM-3$^+$ DC were co-cultured with chemotherapy-exposed dying MC38 cells in the presence of anti-TIM-3 mAb. The TIM-3 blockade increased cytokine mRNA levels in TIM-3$^+$ DC loaded with cisplatin (CDDP)-treated dying MC38 tumor cells (Fig. 8a). The responses induced by anti-TIM-3 mAb were abrogated by pretreatment of dying tumor cells with DNase and RNase, indicating the involvement of nucleic acids. The responses triggered by treatment with supernatant of CDDP-treated MC38 cells, which contain free nucleic acids released from dying tumor cells, were also regulated through TIM-3 regulation of nucleic acid-mediated innate sensing systems (Supplementary Fig. 7a).

Tank-binding kinase-1 (TBK-1) serves as a critical regulator of nucleic acid-mediated innate immunity [7]. Consistent with the importance of TBK-1 in this response, the cytokine induced by dying tumors were suppressed in TBK-1/TNF-α DKO DC compared to those from wild-type or TNF-α KO mice, and anti-TIM-3 mAb had little effects on IFN-β1 expression in TBK-1/TNF-α DKO DC (Fig. 8b). These results indicate the critical contribution of TBK-1 to these responses (Fig. 8b). Consistent with the role of TIM-3 in interfering with HMGB1-mediated nucleic acid sensing pathways, the TIM-3 blockade in TIM-3$^+$ DC loaded with CDDP-treated dying MC38 tumor cells did not increase IFN-β in the presence of anti-HMGB1 neutralizing Ab (Fig. 8c).

I*n vivo* treatment with anti-TIM-3 mAb has little additive effect on CDDP-induced antitumor activity against MC38 tumors in DC-depleted CD11c-DTR mice (Fig. 8d). Thus, the *in vivo* antitumor effects provoked by the combination of TIM-3 blockade and chemotherapy result mainly from the suppression of endogenous DC activities. Interestingly, the depletion of $CD11c^+$ cells alone markedly retarded tumor growth by CDDP treatment, implying that TADC serve as the major suppressor of antitumor responses (Fig. 8d). Furthermore, the antitumor effects triggered by anti-TIM-3 mAb and CDDP were severely impaired in DT-untreated CD11c-DTR mice by combined blockade of type-I IFN and IL-12, suggesting that type-I IFN and IL-12 serves as major effectors to execute antitumor immunity by CDDP and anti-TIM-3 mAb (Supplementary Fig. 7b). Furthermore, CDDP was more effective against MC38 tumors in DT-treated TIM-3-KO/CD11c-DTR mice compared to those without DT, implying that TIM-3 on endogenous DC serves as a major repressor of antitumor responses by chemotherapy (Fig. 8e). Altogether, DC-specific TIM-3 serves as a negative regulator of chemotherapy-induced antitumor responses by circumventing the nucleic acid-mediated innate immune pathways.

DISCUSSION

In this study, we show that tumor-infiltrating DC suppress antitumor immune responses through TIM-3-mediated negative regulation of innate immune responses to nucleic acids. DC-derived TIM-3 interacts with HMGB1 to suppress transport of nucleic acids into endosomal vesicles, thus attenuating the antitumor efficacies of DNA vaccines and cytotoxic chemotherapy by antagonizing nucleic acid-sensing systems. Our findings are the first to provide a novel mechanism by which DC-derived TIM-3 serves as a unique repressor of antitumor responses by targeting nucleic acids that are required for antitumor responses mediated by PRRs (Supplementary Fig. 8).

TIM-3 expression on DC undergoes significant upregulation reaching higher levels and occurring at earlier times than in $CD8^+$ T cells in tumor microenvironments. Indeed, TIM-3 expression on $CD8^+$ T cells increased gradually at later time points of tumor growth, in agreement with recent studies that TIM-3 expression reflects the phenotype of exhausted $CD8^+$ T cells at the chronic phases of tumor burden [16, 39]. These underscore the pivotal role of DC-specific TIM-3 as a negative regulator of nucleic acid-dependent innate immune responses, which may have a critical role in controlling the early stages of tumorigenicity. In this regard, it is of great interest to evaluate further whether myeloid cell-specific TIM-3 plays a role in restraining innate immune responses against viral infections caused by HIV, HCV, *etc*., in

particular at time points prior to the establishment of persistent infection.

Our findings also revealed that DC-specific TIM-3 is indispensable for controlling the *in vivo* antitumor responses mediated by DNA vaccines and chemotherapy, whereas TIM-3 was also highly expressed on tumor-infiltrating myeloid cells other than DC such as TAM. This difference may be due to the differential interactions of DC and TAM with other effector cells such as NK cells, NKT cells, γδ-T cells in the tumor microenvironments. In turn, these differences may have an impact on the extent and quality of antitumor responses elicited by various therapeutic modalities. Whether TIM-3 regulates innate immune responses in different ways depending on the distinct myeloid cell types should be explored in future study.

The interaction between galection-9 and TIM-3 on antigen-presenting cells has been to shown to play a positive role in DC maturation and the cross-priming of tumor-specific T cells [15, 23]. In contrast, TIM-3 on DC has a pro-tumorigenic role and turns down nucleic acid-mediated innate immune responses *via* a galectin-9-independent, but HMGB1-dependent mechanism. We speculate that DC-derived TIM-3 serves as a dual regulator of innate and adaptive immunity depending on the different microenvironments encountered. In endogenous tumor microenvironments, which are characterized by impaired induction of galectin-9 and high expression of HMGB1 (Figure 4C), TIM-3 on DC may suppress innate immune systems by interfering with HMGB1-mediated stimulation of nucleic acid sensing, while TIM-3 maintains

the anergic status of $CD8^+$ T cells in a tumor antigen-specific manner. These coordinated actions of TIM-3 on innate and adaptive responses may systemically incapacitate efficient tumor immunosurveillance during all phases of tumorigenicity. In contrast, while DC-derived TIM-3 may facilitate efficient containment of infectious agents by preferentially interacting with galectin-9-enriched infectious microenvironments, TIM-3 on $CD8^+$ T cells has evolved to suppress antigen-specific responses thus preventing excess tissue inflammation during the recovery phase of post-infection. In this regard, the functional relevance of TIM-3 may be quite different in cancer *vs* infection. In addition, this assumption raises the possibility that proper concentrations of galectin-9 in tumor microenvironments may be crucial for controlling tumorigenesis and to override TIM-3-mediated suppression of innate immune responses. In line with this hypothesis, recent studies have revealed that treatment with exogenous galectin-9 elicits antitumor responses by expanding and activating plasmacytoid DC-like macrophages and NK cells [40].

We also uncovered for the first time that TIM-3 may disrupt the recruitment of nucleic acids into the endosomal pathway by interfering with HMGB1 function, leading to impaired TLR- and cytosolic sensor-mediated innate immune responses. Although tumor cells are mainly composed of mutated or normal "self"-nucleic acids, which are usually sequestered in the nucleus or mitochondria under physiological conditions, tumor microenvironments often

acquire the ability to create an endogenous inflammatory milieu composed of damage-associated molecules such as HMGBs and uric acids [40]. Indeed, we found that HMGB1 was higher in tumor tissues than non-tumor counterparts (Figure 5G). These inflammatory signals could collaborate with tumor-derived nucleic acids to gain access into endosomal vesicles and activate innate immune responses [31, 32]. In this regard, TIM-3 upregulation on TADC may serves as a novel strategy to evade innate immune responses activated at local inflammatory tumor microenvironment.

Notwithstanding our findings that TIM-3 suppresses nucleic acid recruitment to endosome, several scenarios may be considered as additional mechanisms whereby TIM-3 interferes with HMGB1 activation of nucleic acid-mediated responses. First, TIM-3 may affect HMGB1-mediated recognition of nucleic acids by modulating the activities of endosomal endonuclease such as TREX1 or Flap endonuclease 1(FEN1), which are critical for mediating host DNA degradation [42, 43] Alternatively, TIM-3 may inhibit the activities and affinities of other HMGB1-binding partners, such as RAGE and TLR-4, in endosomal vesicles [28, 35]. In addition to their role in nucleic acid-mediated innate immune systems, TIM-3 may also regulate additional functions of HMGB1 including gene transcription, oxidative stress and autophagy [29, 44]. Nevertheless, further investigation will be necessary to clarify the precise mechanisms and physiological relevance of the interplay between TIM-3 and HMGB1 in DC.

An additional novel finding explored in this study is that TIM-3 blockade augmented the antitumor efficacies of anticancer cytotoxic agents in part by augmenting HMGB1-mediated nucleic acid sensing systems. Our observations are consistent with previous findings that tumor-derived nucleic acids could coordinate with danger signals to activate innate immune cells through activation of PRR-mediated pathways [35, 36]. Since TIM-3 also serves as a phosphatidylserine receptor for apoptotic cell engulfment, TIM-3 blockade may also manipulate the phagocytotic pathway in DC, thus modifying the mechanisms for recognition of dying tumor cells. Further investigation should determine the signaling cascades by which TIM-3 on DC controls innate immune pathways when encountering dying tumor cells.

Several lines of evidence underscore the novel role of some cytotoxic drugs in triggering immunogenic cell death, resulting in the triggering of host antitumor immunity against tumor cells through multiple pattern recognition systems [34]. CDDP has been perceived as a "non-immunogenic" chemotherapeutic agent due to the lack of ER stress responses mandatory for triggering DAMP-mediated antigen-specific T cell responses [36, 45]. Instead, CDDP may compromise antitumor innate responses of DC by cooperating with TIM-3-dependent inhibitory pathways. Thus, our findings may provide new evidence that the therapeutic efficacies of even "non-immunogenic" chemotherapy can be harnessed by targeting negative regulatory mechanisms that restrain nucleic acid-mediated innate immune responses.

In summary, we present the first evidence that TIM-3 serves as a negative regulator of nucleic acid-dependent innate immune responses within tumor microenvironments. Given recent findings that TIM-3 serves as a functional marker for leukemia stem cells [46, 47], we propose that TIM-3 is a major sentinel supporting tumor progression by manipulating multiple pathways to create protumorigenic microenvironments. The multiple facets of TIM-3 in tumor biology position pharmacological targeting of TIM-3 as a promising strategy for treating patient refractory to current anticancer modalities.

Methods

Methods and any associated references are available in the online version of the paper.

ACKNOWLEDGEMENTS

We thank Mario Bianchi (San Raffaele University) for providing HMGB1/2-deficient MEF, Osamu Takeuchi and Shizuo Akira (Osaka University) for TBK1/TNF-α DKO mice and Jedd Wolchok (Memorial Sloan-Kettering Cancer Center) for DNA plasmids encoding gp100 and TRP2. We also extend appreciation to Dr. Glenn Dranoff (Harvard Medical School) and Dr. Akinori Takaoka (Hokkaido University) for giving valuable comments to the manuscript. In addition, we wish to extend appreciation to Mr. Tsunaki Yamashina for their assistance with animal care.

This study is partially supported by a Grant-in-Aid for Scientific Research (H. Yagita and M.J.), and Scientific Research for Innovative Area (M.J.) from the Ministry of Education, Culture, Sports, Science and Technology (MEXT), and from the National Cancer Center Research and Development Fund (H. Yagita), and a Grant for Joint Research Program of the Institute for Genetic Medicine, Hokkaido University (M. J., M. H. and H. Yagita), Takeda Science Foundation (M.J.), the Sumitomo Foundation (M.J.), Terumo Life Science Foundation (M.J.), Senshin Medical research Foundation (M.J.), and Japan Leukemia Research Foundation (M.J.).

Author contributions

M.J. and H. Yagita designed the experiments. S.C., M. B., H. A., H. Yoshiyama Y. F., and M. J. prepared reagents and performed the experiments. S. C., M.B., H. A., H. Yoshiyama, Y. F., Y. O., J. C., M. H., T. U., A. T., H. Yagita and M. J. analyzed and discussed the data. I. K. and H. D-A provided clinical samples. H.A., J. G., J. C., M. H. and H. Yagita developed new materials. M. J. was responsible for the overall study design and writing the manuscript.

Author information:

The authors declare no competing financial interests. Correspondence and requests for materials should be addressed to M. J. (jinushi@igm.hokudai.ac.jp).

Figure Legends

Figure 1. TIM-3 expression is upregulated on tumor-associated DC

(a) $CD11c^+$ DC from established tumors (3LL or MC38), tumor-draining lymph nodes (TLN), distal lymph nodes (DLN) or spleens of tumor-bearing mice at 28 days after tumor inoculation were subjected to TIM-3 expression analysis. $CD11c^+$ cells from tumor-free mice served as controls. Representative results (left) and the average of TIM-3^+ cells among $CD11c^+$ cells (right: n=4) are shown. The percentages of TIM-3^+ cells are shown in the right-upper quadrant of each panel. (b) Longitudinal analysis of the percentage of TIM-3-expressing $CD11c^+$ DC or $CD8^+$ T cells after 3LL tumor inoculation. (c) BMDC were treated with 20% supernatant of tumor cells (B16, MC38, 3LL) or directly cocultured with the tumor cells (co-culture: lower panels) for 48 h, and TIM-3 expression was evaluated by flow cytometry. (d) BMDC were treated with 3LL culture supernatants for 48 h. For some instances, the culture supernatants were untreated or pretreated withαVEGFR2, αIL-10 and inhibitors for arginase-I (BEC) (Inhibitors). TIM-3 expression on BMDC was evaluated by flow cytometry, and the representative data (upper) and statistical analysis (n=4: bottom) of percentages of TIM-3^+ $CD11c^+$ cells are shown. (e) TIM-3 expression levels on MoDCs from healthy donors (HD) (n=7) or cancer patients (PT) (n=7), and TADCs from the same patients (n=9) were evaluated

by flow cytometry. Percentages of TIM-3$^+$ CD11c$^+$ cells (top) and representative results (bottom) are shown.

Figure 2. DC-derived TIM-3 suppresses innate responses to nucleic acids

(a) TIM-3$^+$ wild-type BMDC (TIM-3$^+$WT) or TIM-3-deficient (TIM-3 KO) BMDC were stimulated with TLR ligands including peptidoglycan (PGN), poly (I:C), LPS, R848, CpG-ODN1585 (CpG-A) or cytosolic sensor agonists including B-DNA, interferon-stimulatory DNA (ISD), cytosolic poly (I:C) or triphosphate (3p)-RNA. IFN-βlevels were quantified by ELISA. (b) TIM-3$^+$ DC were treated with anti-TIM-3 mAb, siRNA for TIM-3 (TIM-3i) or control siRNA, followed by stimulation with R848, cytosolic poly (I: C), B-DNA for 8 h. IFN-β1 levels were quantified by ELISA. (c) TIM-3$^+$ WT BMDC or TIM-3 KO BMDC were pretreated with αTIM-3 mAb (gray bars) or control Ig (black bars) followed by stimulation with plasmid DNA without insert (control-DNA) or encoding TRP2 (TRP2-DNA) for 12 h. The IFN-β1 proteins were quantified by ELISA. **(**d) MEFs were transfected with TIM-3- or control vectors for 24 h followed by stimulation with B-DNA for 8 h or no treatment (-). IFN-β1, IFN-α4 and IL-6 levels were quantified by RT-PCR. (e) Luciferase assays of lysates from control or TIM-3-transfected HEK293T cells for measuring IRF-3 or NF-κB activities. **(**f) TADC and splenic DC isolated from tumor-bearing mice were pretreated with anti-TIM-3 mAb or control Ig followed

by stimulation with plasmid-DNA for 8 h. IFN-β1 and IL-12 were quantified by RT-PCR. (g) MoDC from healthy donors (HD) or NSCLC patients (PT) and TADC from the same patients were pretreated with control Ig or anti-TIM-3 mAb followed by stimulation with B-DNA. The IFN-β levels were quantified by ELISA.

Figure 3. DC-derived TIM-3 impedes the *in vivo* antitumor activities of DNA

(a) Wild-type C57BL/6 mice (n=4 per group) were inoculated subcutaneously in the flank with B16-F10 melanoma cells, and received intratumor injections of plasmid DNAs encoding murine TRP2 (TRP2-DNA) or CpG-ODN in the presence of control Ig or anti-TIM-3 mAb. (b) Tumors were isolated from untreated mice (NT) or treated with TRP2- or gp100- DNA in the presence of control Ig or anti-TIM-3 mAb. The IFN-β and IL-12 in tumor lysates were quantified by ELISA. (c) CD11c-DTR mice were untreated (DT^-) or treated with DT (DT+). The mice were inoculated subcutaneously with B16-F10 melanoma cells (1×10^5/mouse) along with plasmid DNA in the presence of isotype control Ig or anti-TIM-3 mAb. Tumor growth was measured on the indicated days. (d) Wild-type (WT) or TIM-3-defiecient (TIM-3 KO) BMDCs were adoptively transferred along with DNA plasmids against established B16-F10 tumors in DT treated CD11c-DTR mice (n=5 per group). Results are representative of two independent experiments. (e) B16-F10 tumor cells (1×10^5/mouse) were inoculated into chimeric mice

reconstituted with bone marrow cells from CD11c-DTR and TIM-3 KO mice (TIM-3 KO.CD11c-DTR chimera). The mice were untreated (DT(-)) or treated with DT (DT(+)) to deplete endogenous DC from CD11c-DTR mice 2days before tumor inoculation. The mice were treated with plasmid DNA in the presence of control Ig or anti-TIM-3 mAb on days 8, 10 and 12 after tumor inoculation. Tumor growth was measured on the indicated days.

Figure 4. IFN-I and IL-12 is responsible for anti-TIM-3-mediated antitumor responses

(a-c). CD11c-DTR mice untreated (DT-) (a) or treated with DT (DT+) (b), as well as NOD-SCID (c) mice were inoculated subcutaneously with B16-F10 cells (1 x 10^5/mice) along with intratumoral injection of DNA plasmid in the presence of control Ig or anti-TIM-3 mAb. For some instances, the mice treated with DNA and/or anti-TIM-3 mAb were further treated with neutralizing Ab for type-I IFN receptor (αIFN-IR) and IL-12p40 (αIL-12) or control Ig. Non-treated mice serve as control (NT). The tumor growth was measured on the indicated days. (d, e) cDC, pDC, macrophages, MDSC, NK cells or stromal cells were isolated from the B16 tumors grown in NOD-SCID mice untreated (NT) or treated with DNA(DNA) or DNA and anti-TIM-3 mAb (DNA+αTIM-3). (d) The IFN-β1 and IL-12 levels were measured by RT-PCR. (e) The cells were cocultured with B16 cells at the indicated effector / target (E/T) ratios for 6h. The cytotoxic activities were measured by LDH release assay.

Figure 5. TIM-3 regulates innate responses by a galectin-9 independent way

(a) TIM-3^+ and TIM-3^- BMDC were pretreated with control Ig, recombinant galectin-9 protein (rGal-9) and/or anti-TIM-3 mAb for 30 min followed by stimulation with B-DNA for 8 h. mRNA levels of IFN-β1 and IL-6 were measured by RT-PCR. (b) TIM-3^+ and TIM-3^- BMDC were treated with B-DNA in the presence of control Ig, anti-TIM-3 mAb (αTIM-3) or anti-galectin-9 mAb (αGal-9) for 24 h. The mRNA levels of IFN-β1 and IL-6 were quantified by RT-PCR. (c) Murine galectin-9 mRNA levels in splenic DC, TADC and tumor cells isolated from established tumors (B16 or 3LL), splenic DC from healthy controls (HD) and *in vitro* cultured tumor cells (B16 and 3LL) were quantified by RT-PCR. (d) Galectin-9 levels in B16 tumors as well as normal tissues (thymus, lung, liver, spleen and kidney) from tumor-bearing mice were quantified by RT-PCR. (e) C57BL/6 mice (n=4 per group) were inoculated subcutaneously with B16-F10 melanoma cells (1×10^5 cells/mouse), and received intratumor injections of plasmid DNA in the presence of control Ig or anti-galectin-9 mAb (αGal-9). Tumor growth was measured on the indicated days. (f) MEFs were transfected with TIM-3 or control vectors. After 24 h, the cells were stimulated with B-DNA in the presence of recombinant annexin-V at the indicated concentrations, and the IFN-β1 levels were measured by RT-PCR.

Figure 6. TIM-3 serves as a putative receptor for HMGB1.

(a, b) Fc-fusion proteins containing TIM-3, mutant TIM-3 (Q62A), RAGE or Flt3L were coated onto plastic plates, and biotin-labeled rHMGB1 was added at the indicated concentration. The binding of HMGB1 to each Fc-fusion protein was measured by colorimetric analyses (a). In some instances, control Ig or anti-TIM-3 mAb was added with the rHMGB1 (b). Data are shown as the optical density at 450nm. (c) HMGB1 proteins were coated onto plastic plates, and biotin-labeled B-DNA was loaded in the presence of WT or Q62A TIM-3-Fc or a control Flt3L-Fc as cold competitors at the indicated concentrations. The binding of B-DNA to HMGB1 was measured by colorimetric analyses. (d) $TIM3^+$ or $TIM\text{-}3^-$ DC were cultured with biotin-labeled HMGB1 proteins at the indicated concentrations with or without anti-TIM-3 mAb. Binding of HMGB1 to BMDC was analyzed by flow cytometry. The data are shown as mean fluorescent intensity (MFI). (e) $TIM\text{-}3^+$DC were stained with TIM-3 (green) after loading with rHMGB1 (red). The localization of TIM-3 and HMGB1 was visualized by confocal microscopy. (f) MEFs were transfected with Flag-taged TIM-3 or control vector and loaded with HMGB1 for 30 min in the presence of control Ig or anti-TIM-3 mAb (αTIM-3). The cell lysates were immunoprecipitated with Flag-M2 and then immune-blotted with anti-HMGB1 Ab. The representative data (above) and the densitometry (below) are shown. (g) Murine HMGB1

mRNA levels in tumors as well as normal tissues from tumor-bearing mice were quantified by RT-PCR.

Figure 7. TIM-3 inhibits the recruitment of nucleic acids to endosomes

(a) HMGB1-KO MEFs were transfected with GFP-fused TIM-3, and treated with rHMGB1 or PBS. The localization of B-DNA (red) in the $EEA1^+$ endosomes (blue) was evaluated. (b, c) $TIM\text{-}3^+$WT or TIM-3-KO DC were loaded with rHMGB1 (blue) followed by stimulation with B-DNA. The localization of B-DNA (red) in the $EEA1^+$ endosomes (green) was evaluated (b). Confocal sections (with a z-step of 0.42 μm) were acquired from the bottom to the top of the cells, and vesicles positive for B-DNA or EEA1 were quantified by Meta-Morph software. The values were obtained from 30 cells pooled from three separate experiments (c). (d) The localization of TIM-3 (green) and HMGB1 (blue) in $EEA1^+$ endosomes (red) is visualized by confocal microscopy. (e) Early or late endosomes,, plasma membrane fractions, or total lysates were isolated by sucrose gradient centrifugation from the homogenized samples 2 h after B-DNA treatment, and B-DNA in each fraction were quantified by dot-blot analysis. The contents of EEA1, Rab7 and TfR in each fraction were also evaluated by Western blot. Representative and statistical data (n=3) are shown. (f) HMGB1-deficient or wild-type MEF were transfected with TIM-3 or control vector followed by stimulation with B-DNA or plasmid DNA with or

without rHMGB1. Fold suppression of IFN-β1 by TIM-3 compared to a control gene was evaluated. (g) TIM-3$^+$BMDC were pretreated with control-Ig, anti-TIM-3 mAb or anti-HMGB1 Ab followed by stimulation with B-DNA for 8 h. The IFN-β1 levels were measured by RT-PCR.

Figure 8. TIM-3 impedes the antitumor effects of chemotherapy by interfering with nucleic acid-mediated innate immune responses

(a, b) Apoptosis was induced in MC38 cells by cisplatin (CDDP), and TIM-3$^+$ BMDC were co-cultured with the dying tumor cells (a) in the presence of control Ig or anti-TIM-3 mAb. In some samples, dying tumor cells were treated with DNase and RNase before co-culturing with BMDC. IFN-β1 and IL-12 levels were quantified by RT-PCR. (b) TIM-3$^+$ BMDC from WT, TNF-α KO or TBK1/TNF-α DKO mice were cultured with or without the dying tumor cells in the presence of control Ig or anti-TIM-3 mAb. IFN-β1 levels were quantified by ELISA. (c) TIM-3$^+$ DC were co-cultured with the dying MC-38 cells in the presence of control Ig, anti-TIM-3 mAb, anti-HMGB1 Ab or both. IFN-β1 and IL-12 levels were quantified by RT-PCR. (d) CD11c-DTR mice were untreated (DT-) or treated with DT (DT+). The mice were inoculated subcutaneously with MC38 cells (1×10^5/mouse) along with systemic CDDP in the presence of control Ig or anti–TIM-3 mAb. Non-treated mice served as control (NT). Tumor growth was measured on the indicated days. (e) MC38 cells were inoculated into chimeric mice

reconstituted with bone marrow cells from CD11c-DTR and TIM-3 KO mice (TIM-3 KO / CD11c-DTR chimera) at 1:1 ratio. The mice were untreated (DT-) or treated with DT (DT+) 2 days before tumor inoculation, and then received CDDP on days 8, 10 and 12 after tumor inoculation. Tumor growth was measured on the indicated days.

Online Methods

Mice

C57BL/6, NOD-SCID, and CD11c-DTR transgenic mice were purchased from SCL, Charles River, and Jackson Laboratory respectively. TBK1/TNF-α DKO mice were provided by Prof. Shizuo Akira (Osaka University). TIM-3-deficient mice were generated and used as described [48]. All experiments were conducted under a protocol approved by the animal care committees of Hokkaido University.

Human Samples

The clinical protocols for this project were approved by the Institutional Review Board of Hokkaido University Hospital (Approval number: 10-0114). Tumor tissues and peripheral bloods were obtained from patients with stage-IV NSCLC, colon-carcinoma, gastric-carcinoma and neuroendocrine tumors after written informed consents had been obtained. The cells were isolated by Ficoll-Hypaque density centrifugation and further purified as $CD11c^+$ DCs from tumors and peripheral bloods.

Tumor Cells and MEF

The tumor cells (MC38, B16-F10, 3LL) were obtained from ATCC. Mesenchymal embryonic fibroblasts (MEF) were isolated from wild-type and HMGB1-KO mice.

TIM-3 expression

TIM-3 expression on $CD11c^{low}B220^{+}PDCA1^{+}$ pDC, $CD11c^{high}$ cDC, $F4/80^{+}CD11b^{+}$ macrophages, $CD45^{-}gp38^{+}$ stromal cells, tumor cells in tumor tissues, tumor-draining lymph nodes (TLN) or spleens obtained from tumor-bearing mice were analyzed by flow cytometry using an anti-mouse TIM-3 mAb (RMT3-23) . In primary tumor infiltrates obtained from patients with advanced cancer or in peripheral mononuclear cells, the TIM-3 levels in $CD11c^{+}$ DCs were also examined by flow cytometry using an anti-human TIM-3 mAb (Clone 344823). The *in-vitro* TIM-3 induction in BMDC was examined 24 h after co-culture or treatment with culture supernatant of tumors cells with anti-VEGF-R2 mAb (clone DC101), anti-IL-10 mAb (Clone JES5-16E3), TGF-β-receptor inhibitor (R&D Systems), anti-galectin-9 antibody (clone RG9-35), BEC (Sigma-Aldrich) or 1-MT (Sigma-Aldrich).

Cytokine ELISAs

For analyses of DC cytokine profiles, IFN-β, IFN-α, IL-6 and IL-12 were quantified by ELISA using supernatants obtained from cultured cell according to the manufacturer's instructions (BD Bioscience).

Quantification of cytokine mRNA

The mRNA was isolated from cell lines, tumor infiltrating-DC, TLN or spleens after DNA vaccination and treatment with anti-TIM-3 mAb, or DC from healthy-donors or NSCLC

patients. The cytokine (IFN-β, IFN-α, IL-6 and IL-12) levels were quantified by real-time RT-PCR using SYBR Green Gene Expression Assays (Applied BioSystems).

***In vivo* antitumor effects of DNA adjuvants and anti-TIM-3 mAb**

Wild-type or NOD-SCID mice were injected subcutaneously in the flank with $1x10^5$ B16-F10 melanoma cells, and intra-tumor injections were performed on days 8, 10 and 12 with human gp100, TRP2 or control DNA plasmids, CpG-ODN (Invivogen: 10 μg/mouse) in the presence of anti-TIM-3 mAb (250 μg/mouse) or control Ig.

***In vivo* antitumor effects of DNA adjuvants in CD11c-DTR mice**

CD11c-DTR mice were untreated or treated with DT (4 ng/g body weight, every 2 days from day 2 to day 22) to deplete $CD11c^+$ cells. B16-F10 or MC38 tumor cells ($1x10^5$/mouse) were injected into CD11c-DTR-TG mice and mice were treated with plasmid DNA (50 μg/mouse) and/or anrti-TIM-3 mAb (250 μg/mouse) in the presence or absence of anti-type I IFN-α2 receptor Ab (MMHAR-2: 100 μg/mouse) and anti-IL-12p40 Ab (C17.8: 250 μg/mouse) on days 2, 5 and 8 after tumor inoculation.

Generation of BM mixed chimeric mice

The mixed BM chimeric mice were generated as described previously [49]. In brief, BM-cells isolated from wild-type or TIM-3-deficient mice were mixed with those from CD11c-EGFP-DTR mice at a 1:1 ratio. The BM-cells ($1x10^6$ /mice) were transferred intravenously into

lethally irradiated mice (15 Gy / mice). The efficacy of donor cell reconstitution was evaluated by EGFP-positive populations in peripheral blood 4 weeks after the procedure.

TIM-3 / HMGB1 interaction

Fc-fusion proteins containing TIM-3, mutant TIM-3(Q62A) or Flt3L were used to coat plastic plates and then loaded with biotin-labeled HMGB1 at various concentrations. The binding of biotin-labeled HMGB-1 to each Fc-fusion protein was measured by colorimetric analyses. In some instances, anti-TIM-3 mAb was added with the HMGB-1 protein. Data are shown as the optical density at 450 nm.

Generation of recombinant HMGB1 protein

Deletion series of HMGB1 expressing-vectors: pET28b-HMGB1-Full, pET28b-HMGB1-ΔC-box, pIVEX2.4-HMGB1-ΔA-box, pIVEX2.4-HMGB1-ΔBΔC-box, and pET28b-GST were introduced into BL21(DE3), and the protein were induced and purified as described previously [50].

Immunofluorescence microscopy

BMDC and MEFs cells were stimulated with biotin-labeled HMGB1 and ROX-labeled B-DNA. After fixation, early endosomes were probed by Alexa-Fluor-488 linked anti-EEA1 mAb (C45B10), and internalized HMGB1 were probed by streptavidin-BrilliantViolet-421. Images were obtained using an FV-1000D laser confocal microscope (OLYMPUS). Visualized DNA in

endosomes was quantified using the Meta-Morph software (Universal Imaging, PA). In brief, confocal sections (z-step of 0.42 μm) were acquired from the bottom to the top of the cells, and all sections were projected on one image plane. B-DNA$^+$ or either EEA1$^+$ vesicles were extracted as regions using the "granularity" module and overplayed on the original B-DNA images, and quantified by "measure region" function.

Subcellular fractionation and detection of the B-DNA

TIM-3$^+$ or TIM-3$^-$ DC were incubated with biotin-labeled B-DNA for 90 min. The cells were homogenized with HB$^+$ (250 mM sucrose, 3 mM imidazole pH 7.4, 1 mM EDTA, 30 mM cycloheximide), and the post nuclear supernatants (PNS) were subjected to the sucrose gradient ultracentrifugation at 150,000 g for 1 h with 40.6%, 35%, 25%, and 8% step-gradients. After centrifugation interfaces (8%/25% late-endosome, 25%/35% early-endosome) were collected, and subjected to the immune-blot and DNA dot-blot analysis. To prepare heavy and light plasma membrane fraction, PNS were centrifuged 100,000 g in 30% percoll gradient for 30 min. To detect biotin-labeled B-DNA, fractions were dot-blotted on positively-charged nylon membranes, and B-DNA were probed by streptavidin-HRP.

Evaluation of chemotherapy-mediated antitumor responses

For *in vivo* tumor experiments, CD11c-DTR or BM chimeric mice were challenged subcutaneously in the flank with MC38 cells ($1x10^5$), and intra-peritoneal injections were

performed on days 8, 10 and 12 with cisplatin (CDDP) (10 mg/kg), anti-TIM-3 mAb (250 μg/mouse), IFN-IR Ab (100 μg/mouse) or anti-IL-12p40 Ab (250 μg/mouse). For *in vitro* assays, TIM-3^+ BMDCs were co-cultured with the apoptotic tumor cells pre-treated with DNase and RNase (10 μg/ml: Invitrogen) in the presence of anti-TIM-3 mAb, anti-HMGB1 Ab or control Ig, and the cytokine levels were evaluated by RT-PCR.

Statistical analyses

Statistical analyses were performed using the paired Student's *t*-test, and $p<0.05$ was considered statistically significant. *$p<0.05$, **$p<0.01$, ns: not significant.

REFERENCES

1. Hanahan, D. & Weinberg, R.A. Hallmarks of cancer: the next generation. *Cell* **144**, 646-674 (2011).

2. Schreiber, R.D., Old, L.J. & Smyth, M.J. Cancer immunoediting: integrating immunity's roles in cancer suppression and promotion. *Science* **331**, 1565-1570 (2011).

3. Bindea, G., Mlecnik, B., Fridman, W.H., Pages, F. & Galon, J. Natural immunity to cancer in humans. *Curr. Opin. Immunol.* **22**, 215-222 (2010).

4. Dougan, M. & Dranoff, G. Immune therapy for cancer. *Annu. Rev. Immunol.* **27,** 83-117 (2009).

5. Rabinovich, G.A., Gabrilovich, D. & Sotomayor, E.M. Immunosuppressive strategies that are mediated by tumor cells. *Annu. Rev. Immunol.* **25**, 267-296 (2007).

6. Drake, C.G., Jaffee, E. & Pardoll, D.M. Mechanisms of immune evasion by tumors. *Adv. Immunol.* **90**, 51-81 (2006).

7. Takeuchi, O. & Akira, S. Pattern recognition receptors and inflammation. *Cell* **140**, 805-820 (2010).

8. Steinman, R.M. & Banchereau, J. Taking dendritic cells into medicine. *Nature* **449**, 419-426 (2007).

9. Peng, G., *et al.* Toll-like receptor 8-mediated reversal of CD4+ regulatory T cell function.

Science **309**, 1380-1384 (2005).

10. Poeck, H., *et al.* 5'-Triphosphate-siRNA: turning gene silencing and Rig-I activation against melanoma. *Nat. Med.* **14**, 1256-1263(2008).
11. Besch, R., *et al.* Proapoptotic signaling induced by RIG-I and MDA-5 results in type I interferon-independent apoptosis in human melanoma cells. *J. Clin. Invest.* **119**, 2399-2411 (2009) .
12. Kuchroo, V.K., Dardalhon, V., Xiao, S. & Anderson, A.C. New roles for TIM family members in immune regulation. *Nat. Rev. Immunol.* **8**, 577-580 (2008).
13. Sanchez-Fueyo, A., *et al.* Tim-3 inhibits T helper type 1-mediated auto- and alloimmune responses and promotes immunological tolerance. *Nat. Immunol.* **4**, 1093-1101 (2003).
14. Zhu, C., *et al.* The Tim-3 ligand galectin-9 negatively regulates T helper type 1 immunity. *Nat. Immunol.* **6**, 1245-1252 (2005).
15. Anderson, A.C., *et al.* Promotion of tissue inflammation by the immune receptor Tim-3 expressed on innate immune cells. *Science* **318**, 1141-1143 (2007).
16. Zhou, Q., *et al.* Coexpression of Tim-3 and PD-1 identifies a CD8+ T-cell exhaustion phenotype in mice with disseminated acute myelogenous leukemia. *Blood* **117**, 4501-4510 (2011).
17. Munn, D.H., *et al.* Potential regulatory function of human dendritic cells expressing

indoleamine 2,3-dioxygenase. *Science* **297**, 1867-1870 (2002).

18. Norian, L.A., *et al.* Tumor-infiltrating regulatory dendritic cells inhibit CD8+ T cell function via L-arginine metabolism. *Cancer Res*. **69**, 3086-3094 (2009).

19. Gabrilovich, D.I., *et al.* Production of vascular endothelial growth factor by human tumors inhibits the functional maturation of dendritic cells. *Nat. Med.* **2**, 1096-1103(1996).

20. Bowne, W.B., *et al.* Coupling and uncoupling of tumor immunity and autoimmunity. *J. Exp. Med.* **190**, 1717-1722 (1999).

21. Ngiow, S.F., *et al.* Anti-TIM3 antibody promotes T cell IFN-gamma-mediated antitumor immunity and suppresses established tumors. *Cancer Res.* **71**, 3540-3551 (2011).

22. Drobits, B., *et al.* Imiquimod clears tumors in mice independent of adaptive immunity by converting pDCs into tumor-killing effector cells. *J. Clin. Invest.* **22**, 575-585 (2012).

23. Nagahara, K., *et al.* Galectin-9 increases Tim-3+ dendritic cells and CD8+ T cells and enhances antitumor immunity via galectin-9-Tim-3 interactions. *J. Immunol.* **181**, 7660-7669 (2008).

24. Jayaraman, P., *et al.* Tim3 binding to galectin-9 stimulates antimicrobial immunity. *J. Exp. Med.* **207**, 2343-2354 (2008).

25. Dardalhon, V., *et al.* Tim-3/galectin-9 pathway: regulation of Th1 immunity through promotion of CD11b+Ly-6G+ myeloid cells. *J. Immunol.* **185**, 1383-1392 (2010)

26. Nakayama, M., *et al.* Tim-3 mediates phagocytosis of apoptotic cells and cross-presentation. *Blood* **113**, 3821-3830 (2009).

27. DeKruyff, R.H., *et al.* T cell/transmembrane, Ig, and mucin-3 allelic variants differentially recognize phosphatidylserine and mediate phagocytosis of apoptotic cells. *J. Immunol.* **184**, 1918-1930 (2010).

28. Ablasser, A., *et al.* RIG-I-dependent sensing of poly(dA:dT) through the induction of an RNA polymerase III-transcribed RNA intermediate. *Nat. Immunol.* **10**, 1065-1072 (2009).

29. Sims, G.P., Rowe, D.C., Rietdijk, S.T., Herbst, R. & Coyle, A.J. HMGB1 and RAGE in inflammation and cancer. *Annu. Rev. Immunol.* **28**, 367-388 (2010).

30. Tian, J., *et al.* Toll-like receptor 9-dependent activation by DNA-containing immune complexes is mediated by HMGB1 and RAGE. *Nat. Immunol.* **8**, 487-496 (2007).

31. Yanai, H., *et al.* HMGB proteins function as universal sentinels for nucleic-acid-mediated innate immune responses. *Nature* **462**, 99-103 (2009).

32. Cao, E., *et al.* T cell immunoglobulin mucin-3 crystal structure reveals a galectin-9-independent ligand-binding surface. *Immunity* **26**, 311-321(2007).

33. Santiago, C., *et al.* Structures of T cell immunoglobulin mucin protein 4 show a metal-Ion-dependent ligand binding site where phosphatidylserine binds. *Immunity* **27**, 941-951 (2007).

34. Blasius, A. L. and Beutler, B. Intracellular toll-like receptors. Immunity. 32, 305-315 (2010).

35. Fujioka, Y., *et al.* The Ras-PI3K signaling pathways is involved in clathrin-independnet endocytosis and the internalization of influenza viruses. *PLoS ONE* **6**, e16324 (2011).

36. Green, D.R., Ferguson, T., Zitvogel, L. & Kroemer, G. Immunogenic and tolerogenic cell death. *Nat. Rev. Immunol.* **9**, 353-363 (2009).

37. Apetoh, L., *et al.* Toll-like receptor 4-dependent contribution of the immune system to anticancer chemotherapy and radiotherapy. *Nat. Med.* **13**, 1050-1059 (2007).

38. Lin, Y., *et al.* Effective post-transplant antitumor immunity is associated with TLR-stimulating nucleic acid-immunoglobulin complexes in humans. *J. Clin. Invest.* **121**, 1574-1584 (2011).

39. Jones, R.B., *et al.* Tim-3 expression defines a novel population of dysfunctional T cells with highly elevated frequencies in progressive HIV-1 infection. *J. Exp. Med.* **205**, 2763-2779 (2008).

40. Nobumoto, A., *et al.* Galectin-9 expands unique macrophages exhibiting plasmacytoid dendritic cell-like macrophages that activate NK cells in tumor-bearing mice. *Clin. Immunol.* **130**, 322-330 (2009).

41. Grivennikov, S. I., Greten, F. R. & Karin, M. Immunity, inflammation, and cancer. *Cell* **140**, 883-899 (2010).

42. Stetson, D.B., Ko, J.S., Heidmann, T. & Medzhitov, R. Trex1 prevents cell-intrinsic

initiation of autoimmunity. *Cell* **134**, 587-598 (2008).

43. Zheng, L., *et al.* Fen1 mutations results in autoimmunity, chronic inflammation and cancers. *Nat. Med.* **13**, 812-819 (2007).

44. Anderson, U. & Tracy, K.J. HMGB1 in a therapeutic target for sterile inflammation and infection. *Annu. Rev. Immunol.* **29**, 139-162 (2011).

45. Michaud, M., *et al.* Autophagy-dependent anticancer immune responses induced by chemotherapeutic agents in mice. *Science* **334**, 1573-1577 (2011).

46. Kikushige, Y., *et al.* TIM-3 is a promising target to selectively kill acute myeloid leukemia stem cells. *Cell Stem Cell* **7**, 708-717 (2010).

47. Jan, M., *et al.* Prospective separation of normal and leukemic stem cells based on differential expression of TIM3, a human acute myeloid leukemia stem cell marker. *Proc. Natl. Acad. Sci. US A.* **108**, 5009-5014 (2011).

48. ,Sabatos, C.A., *et al.* Interaction of Tim-3 and Tim-3 ligand regulates T helper type 1 responses and induction of peripheral tolerance. *Nat. Immunol.* **4,** 1102-1110 (2003).

49. Kinnebrew, M.A., *et al.* Interleukin 23 production by intestinal CD103+ CD11b+ dendritic cells in response to bacterial flagellin enhances mucosal innate immune defense. *Immunity* **36,** 276-287 (2012).

50. Najima, Y., *et al*. High mobility group protein-B1 interacts with sterol regulatory element-

binding proteins to enhance their DNA binding. *J. Biol. Chem.* **280**, 27523-27532 (2005).

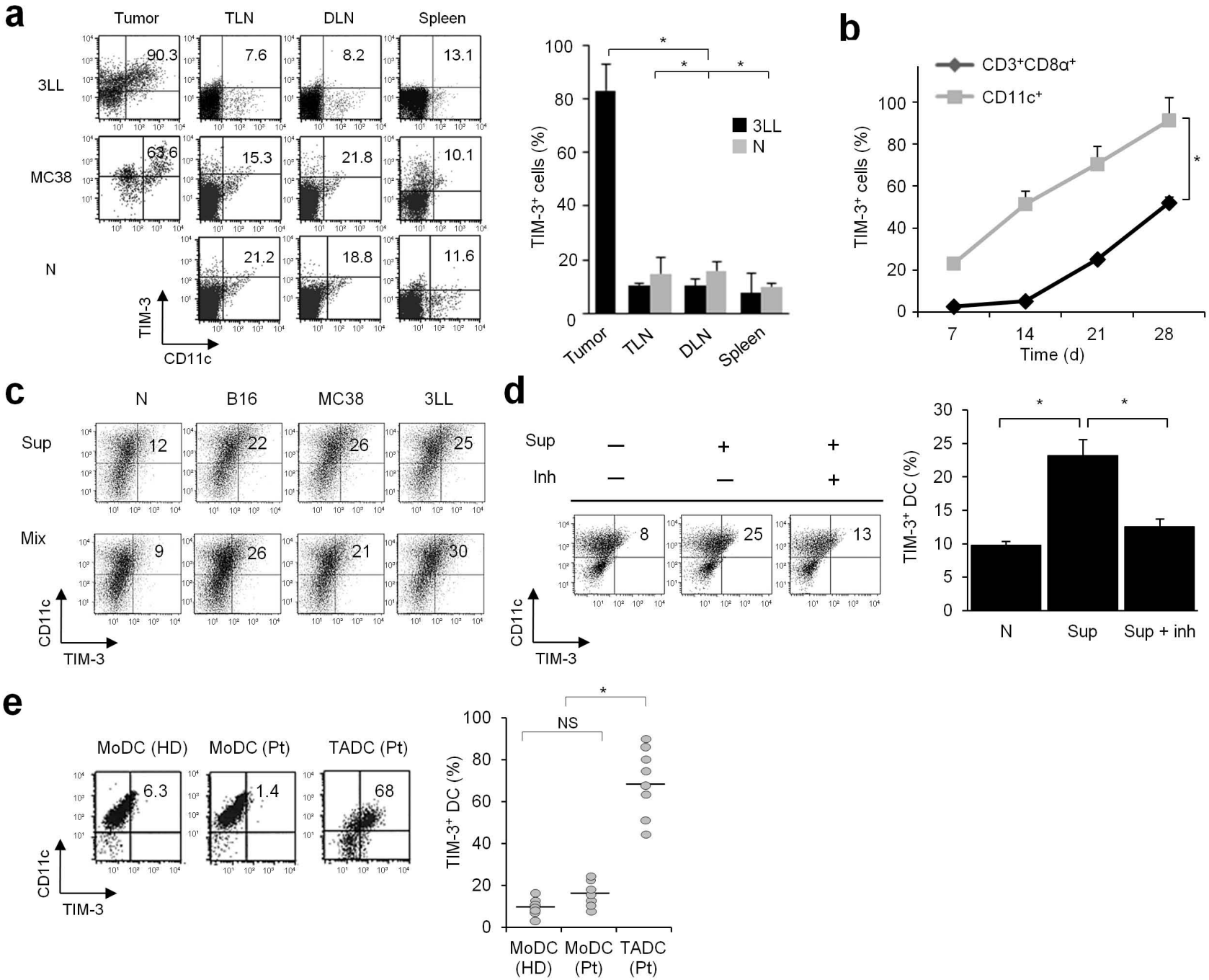
a
Tumor
TLN
DLN
Spleen
3LL
MC38
N
90.3
7.6
8.2
13.1
63.6
15.3
21.8
10.1
21.2
18.8
11.6
TIM-3
CD11c
TIM-3+ cells (%)
3LL
N
Tumor
TLN
DLN
Spleen
b
CD3+CD8α+
CD11c+
TIM-3+ cells (%)
Time (d)
c
N
B16
MC38
3LL
Sup
Mix
12
22
26
25
9
26
21
30
CD11c
TIM-3
d
Sup
Inh
8
25
13
TIM-3+ DC (%)
N
Sup
Sup + inh
e
MoDC (HD)
MoDC (Pt)
TADC (Pt)
6.3
1.4
68
CD11c
TIM-3
NS
TIM-3+ DC (%)
MoDC (HD)
MoDC (Pt)
TADC (Pt)

Figure 1

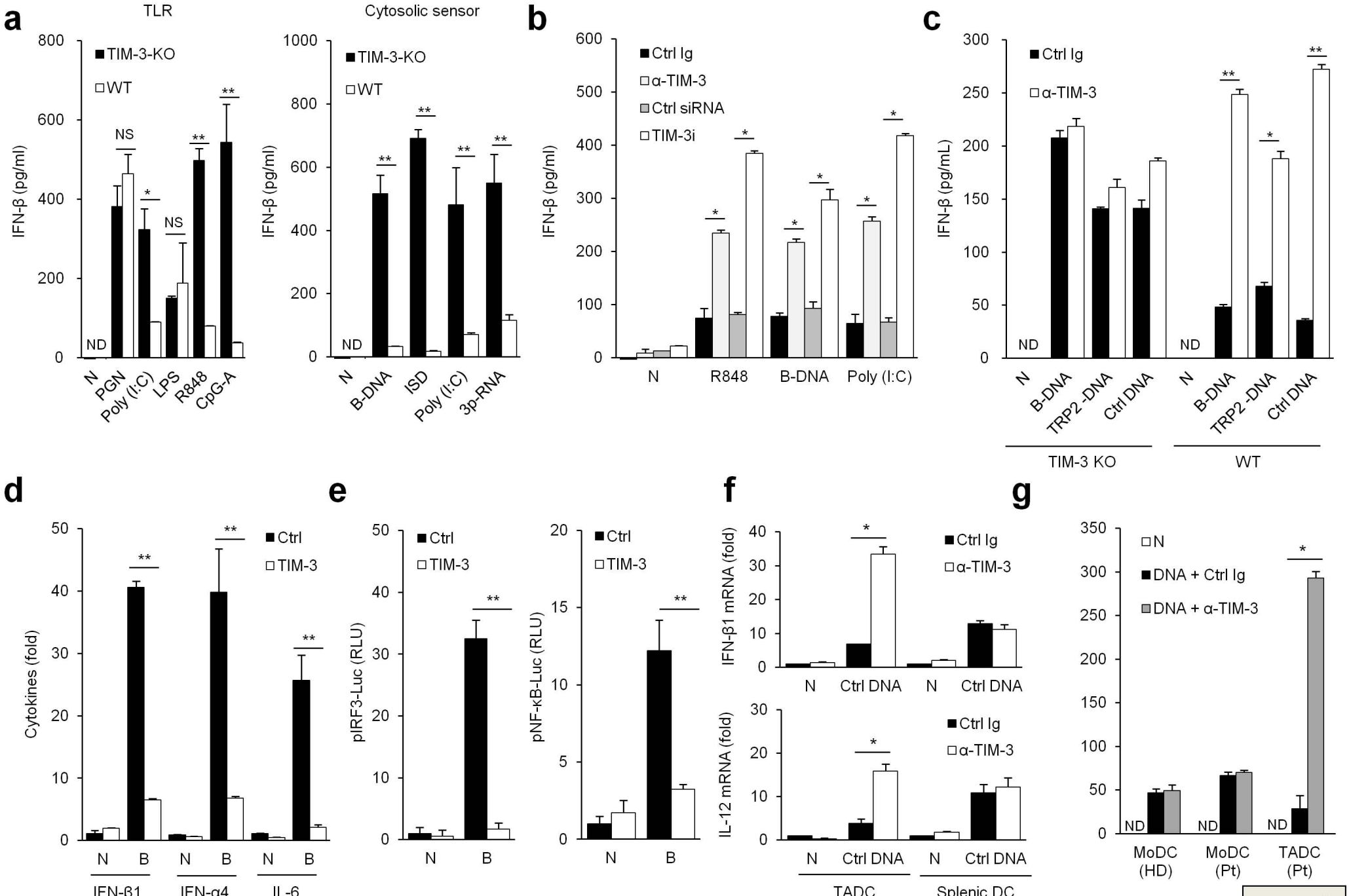
a
TLR
Cytosolic sensor
TIM-3-KO
WT
IFN-β (pg/ml)
ND
NS
N
PGN
Poly (I:C)
LPS
R848
CpG-A
B-DNA
ISD
3p-RNA
b
Ctrl Ig
α-TIM-3
Ctrl siRNA
TIM-3i
N
R848
B-DNA
Poly (I:C)
c
Ctrl Ig
α-TIM-3
IFN-β (pg/mL)
B-DNA
TRP2 -DNA
Ctrl DNA
TIM-3 KO
WT
d
Ctrl
TIM-3
Cytokines (fold)
N
B
IFN-β1
IFN-α4
IL-6
e
pIRF3-Luc (RLU)
pNF-κB-Luc (RLU)
f
IFN-β1 mRNA (fold)
IL-12 mRNA (fold)
Ctrl DNA
TADC
Splenic DC
g
N
DNA + Ctrl Ig
DNA + α-TIM-3
MoDC (HD)
MoDC (Pt)
TADC (Pt)

Figure 2

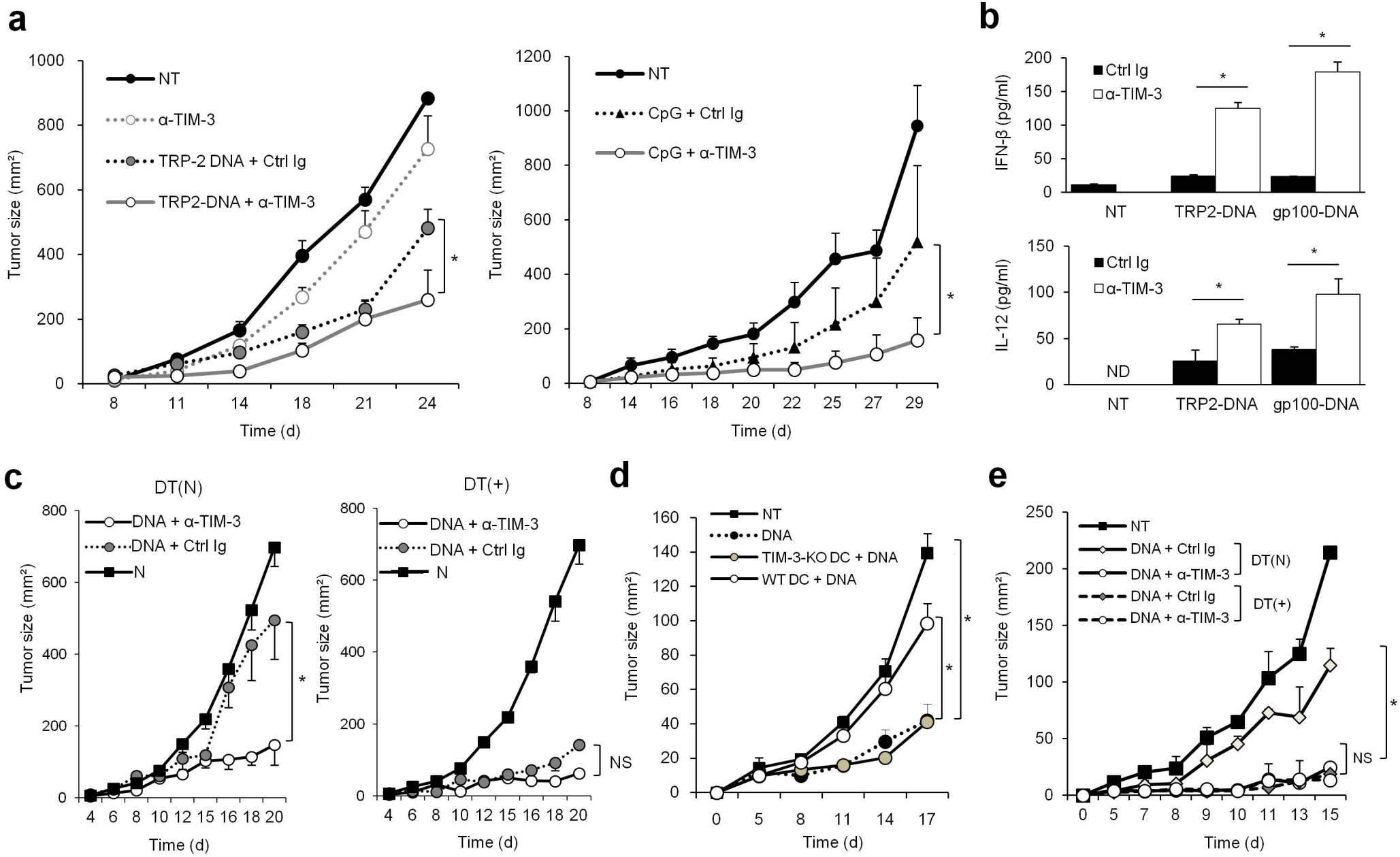
a
Tumor size (mm²)
Time (d)
NT
α-TIM-3
TRP-2 DNA + Ctrl Ig
TRP2-DNA + α-TIM-3
CpG + Ctrl Ig
CpG + α-TIM-3
b
IFN-β (pg/ml)
IL-12 (pg/ml)
Ctrl Ig
α-TIM-3
ND
NT
TRP2-DNA
gp100-DNA
c
DT(N)
DT(+)
DNA + α-TIM-3
DNA + Ctrl Ig
N
NS
d
NT
DNA
TIM-3-KO DC + DNA
WT DC + DNA
e
DNA + Ctrl Ig
DNA + α-TIM-3
DT(N)
DT(+)

Figure 3

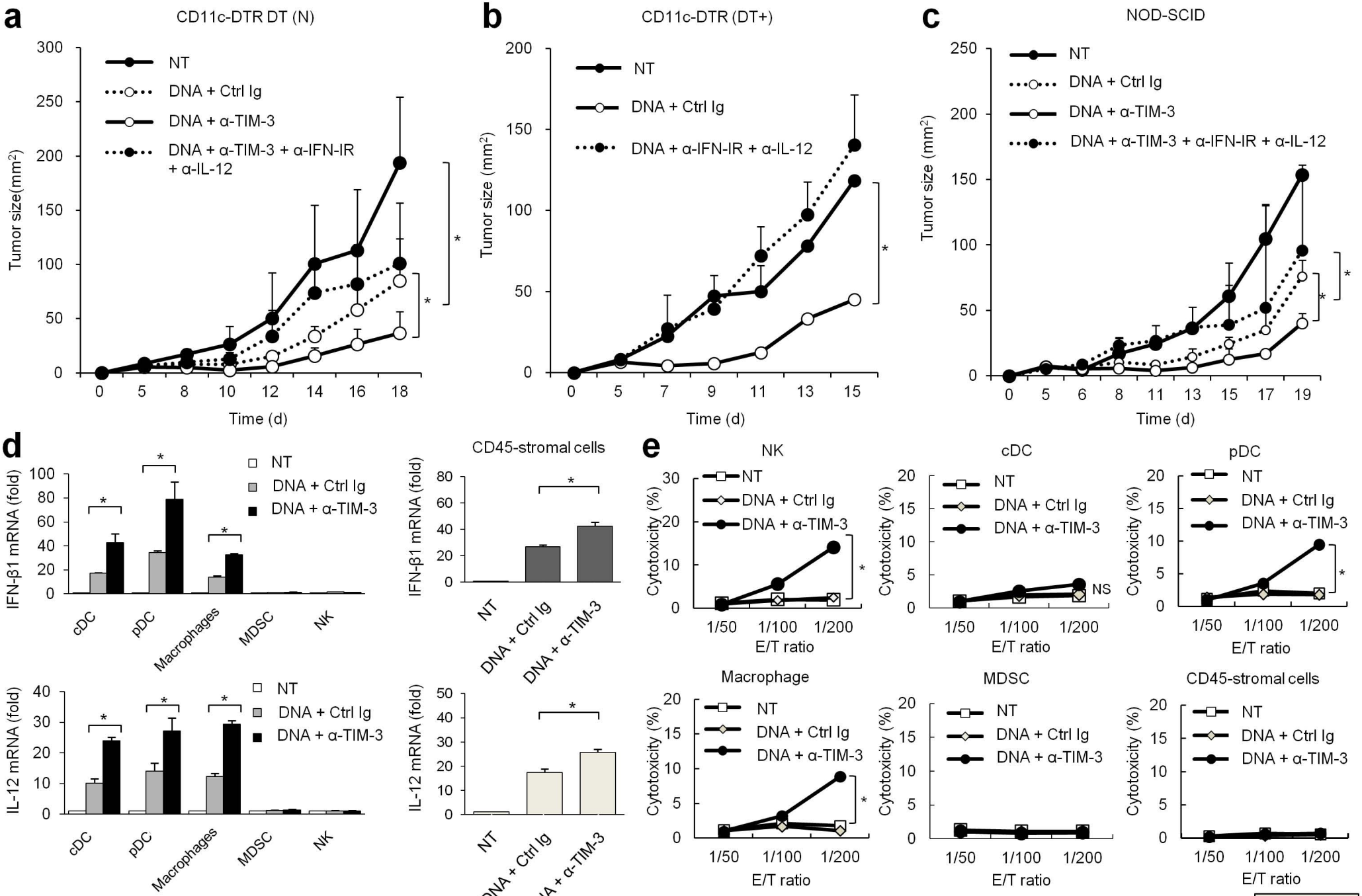
a
CD11c-DTR DT (N)
NT
DNA + Ctrl Ig
DNA + α-TIM-3
DNA + α-TIM-3 + α-IFN-IR + α-IL-12
Tumor size(mm2)
Time (d)
b
CD11c-DTR (DT+)
NT
DNA + Ctrl Ig
DNA + α-IFN-IR + α-IL-12
Tumor size (mm2)
Time (d)
c
NOD-SCID
NT
DNA + Ctrl Ig
DNA + α-TIM-3
DNA + α-TIM-3 + α-IFN-IR + α-IL-12
Tumor size (mm2)
Time (d)
d
IFN-β1 mRNA (fold)
NT
DNA + Ctrl Ig
DNA + α-TIM-3
cDC
pDC
Macrophages
MDSC
NK
CD45-stromal cells
IL-12 mRNA (fold)
e
NK
cDC
pDC
Macrophage
MDSC
CD45-stromal cells
Cytotoxicity (%)
E/T ratio
1/50
1/100
1/200
NS

Figure 4

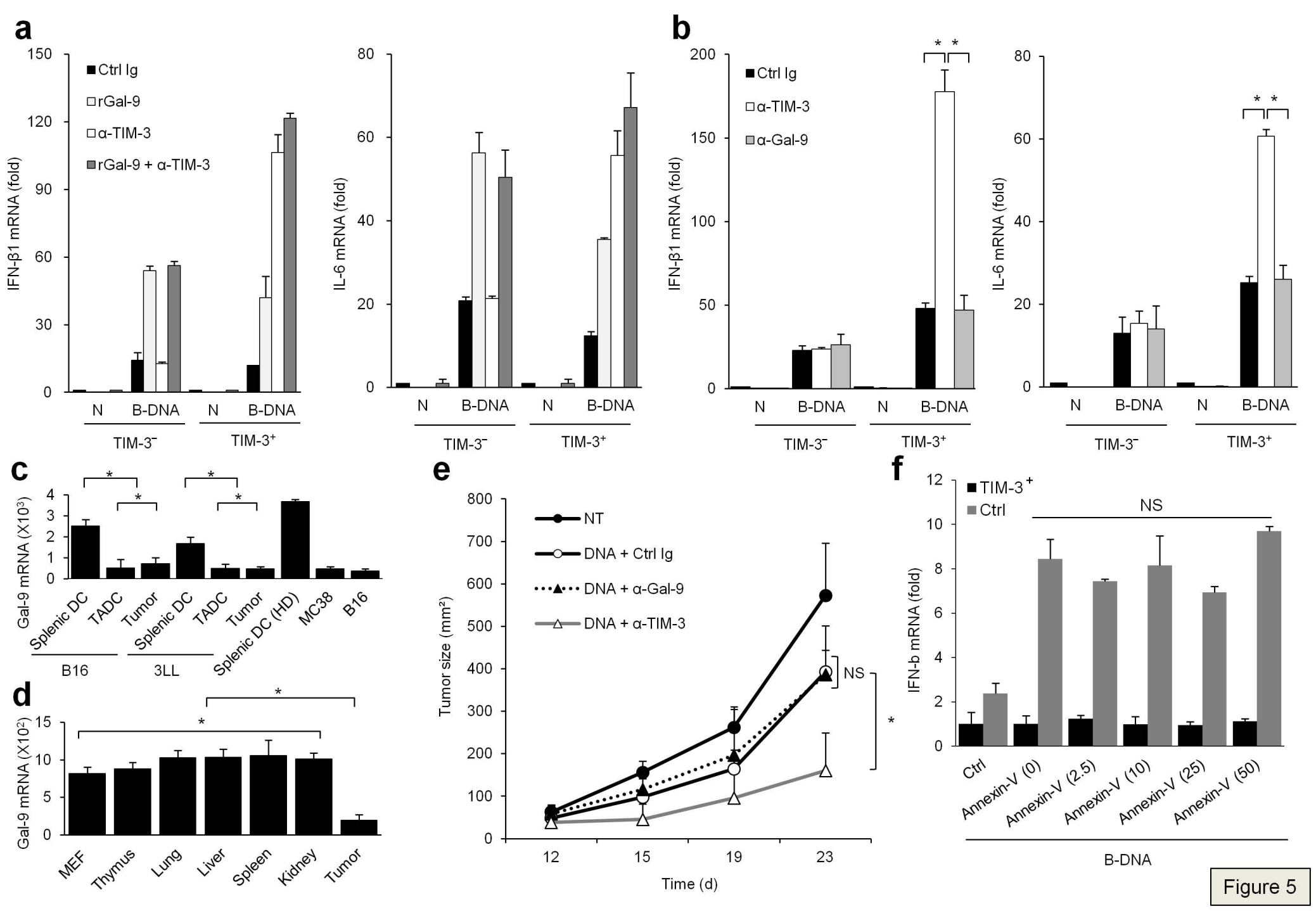
a
Ctrl Ig
rGal-9
α-TIM-3
rGal-9 + α-TIM-3
IFN-β1 mRNA (fold)
IL-6 mRNA (fold)
N
B-DNA
TIM-3⁻
TIM-3⁺
b
Ctrl Ig
α-TIM-3
α-Gal-9
c
Gal-9 mRNA (X10³)
Splenic DC
TADC
Tumor
Splenic DC
TADC
Tumor
Splenic DC (HD)
MC38
B16
B16
3LL
d
Gal-9 mRNA (X10²)
MEF
Thymus
Lung
Liver
Spleen
Kidney
Tumor
e
NT
DNA + Ctrl Ig
DNA + α-Gal-9
DNA + α-TIM-3
Tumor size (mm²)
Time (d)
NS
f
TIM-3⁺
Ctrl
NS
IFN-b mRNA (fold)
Ctrl
Annexin-V (0)
Annexin-V (2.5)
Annexin-V (10)
Annexin-V (25)
Annexin-V (50)
B-DNA

Figure 5

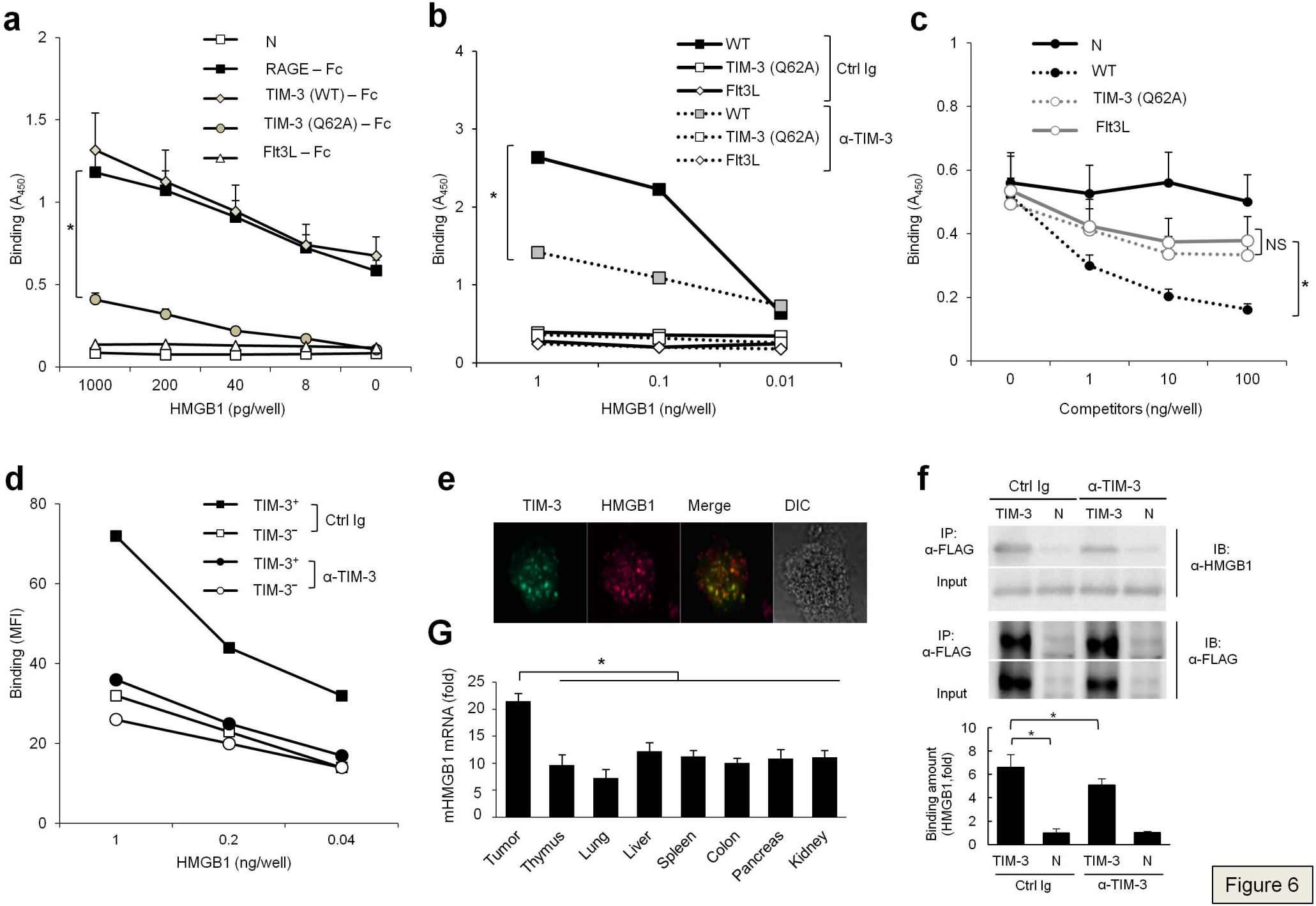
a
N
RAGE – Fc
TIM-3 (WT) – Fc
TIM-3 (Q62A) – Fc
Flt3L – Fc
Binding (A450)
HMGB1 (pg/well)
1000
200
40
8
0
b
WT
TIM-3 (Q62A)
Flt3L
Ctrl Ig
α-TIM-3
Binding (A450)
HMGB1 (ng/well)
1
0.1
0.01
c
N
WT
TIM-3 (Q62A)
Flt3L
NS
Binding (A450)
Competitors (ng/well)
d
TIM-3+
TIM-3−
Ctrl Ig
α-TIM-3
Binding (MFI)
HMGB1 (ng/well)
e
TIM-3
HMGB1
Merge
DIC
G
mHMGB1 mRNA (fold)
Tumor
Thymus
Lung
Liver
Spleen
Colon
Pancreas
Kidney
f
Ctrl Ig
α-TIM-3
IP: α-FLAG
Input
IB: α-HMGB1
IB: α-FLAG
Binding amount (HMGB1,fold)

Figure 6

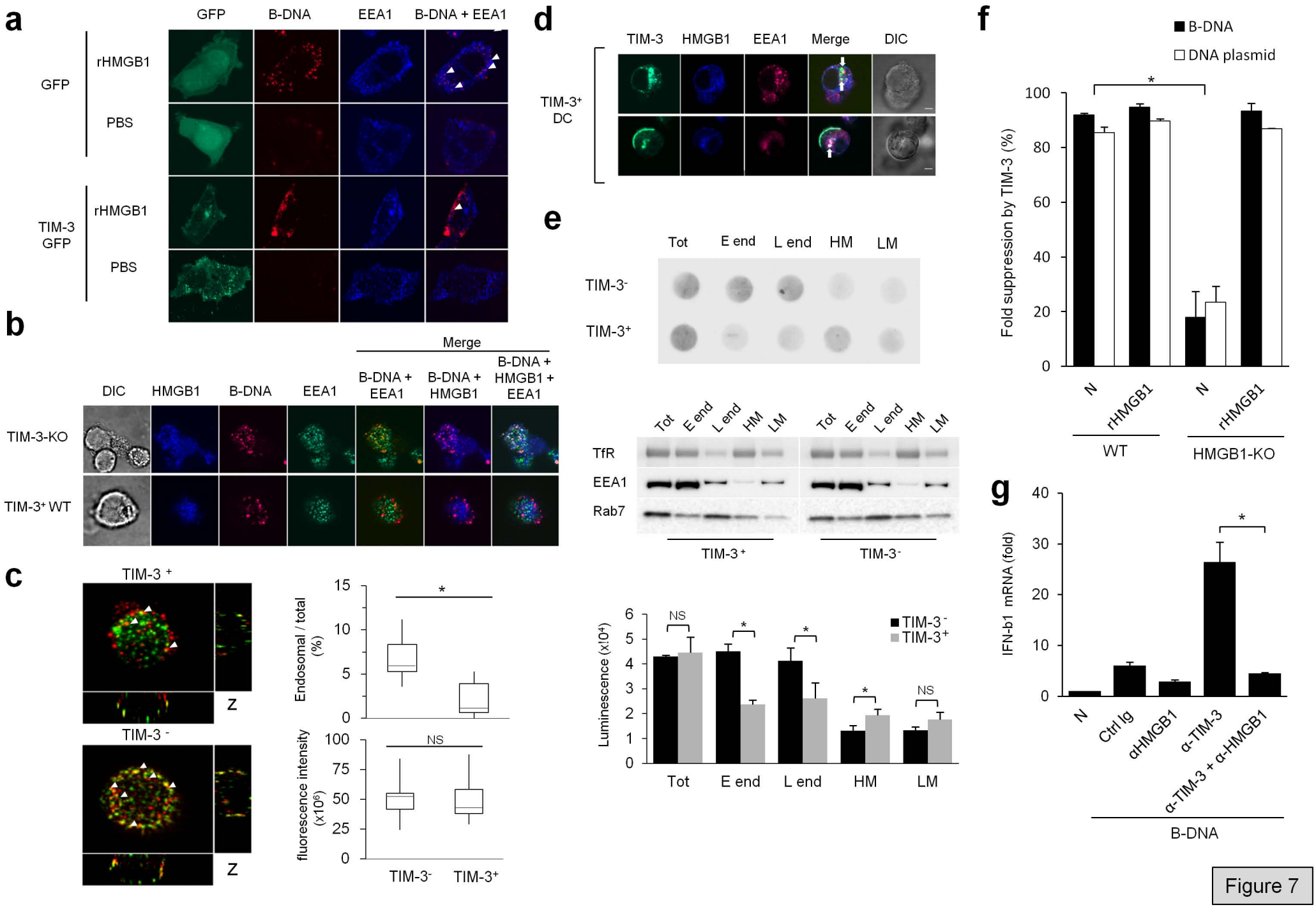
a
GFP
B-DNA
EEA1
B-DNA + EEA1
GFP
rHMGB1
PBS
TIM-3 GFP
rHMGB1
PBS
b
Merge
DIC
HMGB1
B-DNA
EEA1
B-DNA + EEA1
B-DNA + HMGB1
B-DNA + HMGB1 + EEA1
TIM-3-KO
TIM-3+ WT
c
TIM-3 +
Z
TIM-3 -
Z
Endosomal / total (%)
fluorescence intensity (x10⁶)
NS
TIM-3-
TIM-3+
d
TIM-3
HMGB1
EEA1
Merge
DIC
TIM-3+ DC
e
Tot
E end
L end
HM
LM
TIM-3-
TIM-3+
TfR
EEA1
Rab7
TIM-3 +
TIM-3-
Luminescence (x10⁴)
NS
TIM-3 -
TIM-3+
Tot
E end
L end
HM
LM
f
B-DNA
DNA plasmid
Fold suppression by TIM-3 (%)
N
rHMGB1
N
rHMGB1
WT
HMGB1-KO
g
IFN-b1 mRNA (fold)
N
Ctrl Ig
αHMGB1
α-TIM-3
α-TIM-3 + α-HMGB1
B-DNA

Figure 7

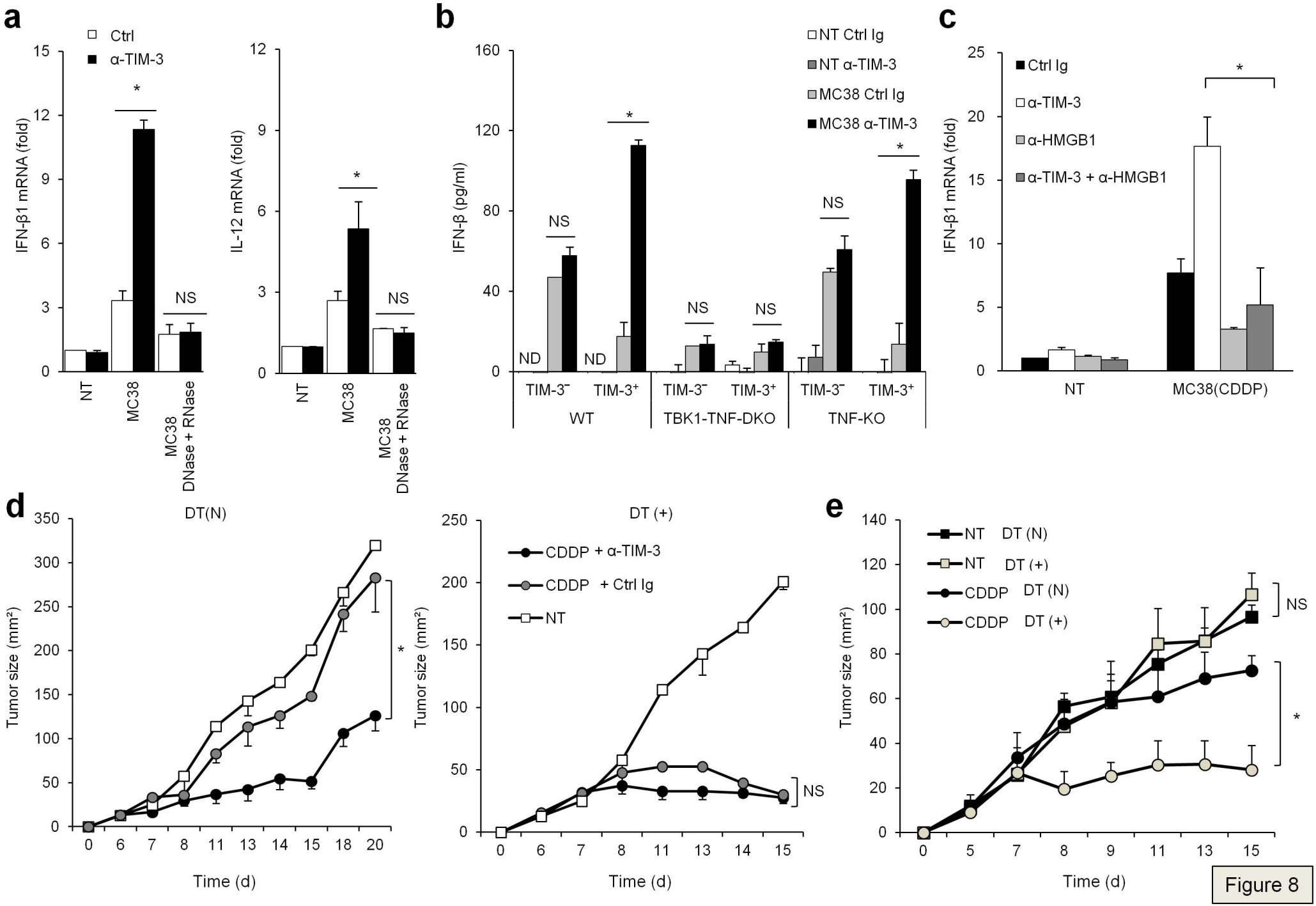
a
Ctrl
α-TIM-3
IFN-β1 mRNA (fold)
IL-12 mRNA (fold)
NT
MC38
MC38 DNase + RNase
NS
b
NT Ctrl Ig
NT α-TIM-3
MC38 Ctrl Ig
MC38 α-TIM-3
IFN-β (pg/ml)
ND
TIM-3⁻
TIM-3⁺
WT
TBK1-TNF-DKO
TNF-KO
c
Ctrl Ig
α-TIM-3
α-HMGB1
α-TIM-3 + α-HMGB1
IFN-β1 mRNA (fold)
NT
MC38(CDDP)
d
DT(N)
DT (+)
CDDP + α-TIM-3
CDDP + Ctrl Ig
NT
Tumor size (mm²)
Time (d)
e
NT DT (N)
NT DT (+)
CDDP DT (N)
CDDP DT (+)
Tumor size (mm²)
Time (d)

Figure 8